

Ilona Mäkinen

**COMPUTATIONAL MODELLING OF
BRAIN ENERGY METABOLISM IN
SCHIZOPHRENIA**
Insights from post-mortem RNA sequencing data

Faculty of Medicine and Health Technology
Master's Thesis
November 2024

ABSTRACT

Ilona Mäkinen: Computational modelling of brain energy metabolism in schizophrenia: insights from post-mortem RNA sequencing data

Master's Thesis

Tampere University

Master's Programme in Biotechnology and Biomedical Engineering

Supervisor(s): Dr. Tuomo Mäki-Marttunen and Doc. Marja-Leena Linne

Examiners: Dr. Tuomo Mäki-Marttunen and Prof. Matti Nykter

November 2024

Schizophrenia is a complex psychiatric disorder characterized by a wide variety of symptoms such as hallucinations, delusions, lack of pleasure and problems in attention and memory. The aetiology of the disorder is not fully understood, but dysregulation of multiple neurotransmitter systems as well as genetic and environmental factors contribute to the pathology of schizophrenia. Furthermore, schizophrenia is associated with disruptions in brain energy metabolism. Since signalling activities of the brain require constant energy supply, problems in brain energy metabolism can cause abnormalities in the synaptic activity.

This thesis investigated the connection between the expression of cytosolic energy metabolism genes and the concentrations of central energy metabolites in neurons and astrocytes. First, a differential expression (DE) analysis was performed to study the gene expression differences between schizophrenia patients and healthy individuals. The DE analysis utilized post-mortem bulk RNA sequencing data from the prefrontal cortex (PFC) and the anterior cingulate cortex (ACC). After the DE analysis, cell-type specific gene expressions were imputed for neurons and astrocytes. Finally, a computational model of brain energy metabolism was used to simulate the gene expression changes. The aim of the simulations was to study how the gene expression alterations influence the concentrations of key metabolites.

The DE analysis revealed that there are 23 differentially expressed cytosolic energy metabolism genes in the PFC and nine in the ACC. Moreover, around two thirds of the DE genes were downregulated in schizophrenia in both brain areas. Yet, the simulation results showed that altered expression of most of the genes had no significant effects on concentrations of the considered metabolites. However, decreased expression of neuronal PFKM gene in the PFC caused significant changes in all but one metabolite in both neurons and astrocytes. In addition, decreased neuronal LDHB in the ACC caused smaller yet significant changes in a few neuronal metabolites.

In conclusion, the results obtained in this thesis provide additional support for brain energy metabolism dysregulation in schizophrenia. The DE analysis results suggest that dysregulation of brain energy metabolism is region-specific, and that the dysregulation is stronger in the PFC than the ACC. Lastly, the simulation results show that most cytosolic energy metabolism genes do not alone have the power to significantly alter the concentrations of central energy metabolites. This suggests that these gene expression alterations do not alone cause the complex disruptions of energy metabolism in schizophrenia.

Keywords: Schizophrenia, neuron, astrocyte, brain energy metabolism, computational modelling, differential expression analysis

The originality of this thesis has been checked using the Turnitin OriginalityCheck service.

DECLARATION ON THE USE OF ARTIFICIAL INTELLIGENCE (AI)

The AI tools used in my thesis and the purpose of their use has been described below:

Name of the tool: ChatGPT, versions GPT-4 and GPT-4o.

Purpose of use: Improving sentence structure, checking the grammar and finding suitable R functions and packages for the data analysis.

I am aware that I am totally responsible for the entire content of the thesis, including the parts generated by AI, and accept the responsibility for any violations of the ethical standards of publications.

PREFACE

This master's thesis was carried out in the Computational Neuroscience research group in Tampere university, Finland. First, I want to thank my supervisors Academy Research Fellow, Dr. Tuomo Mäki-Marttunen and Docent Marja-Leena Linne for excellent guidance and support, and for offering me great academic opportunities and experiences. I also want to thank the rest of the Computational Neuroscience group for all the insightful meetings and conversations. Lastly, thank you to all my friends and family for the support and encouragement, and a special thank you for my godson for always making me smile throughout this project.

Tampere, 6 November 2024

Ilona Mäkinen

CONTENTS

ABSTRACT	1
1.INTRODUCTION	1
2.LITERATURE REVIEW.....	3
2.1 Schizophrenia.....	3
2.1.1 Genetics and environmental factors.....	4
2.1.2 Dopamine	4
2.1.3 Glutamate, GABA and excitatory/inhibitory balance	5
2.1.4 Dysfunction of neural circuits and connection to symptoms	7
2.1.5 Astrocytes.....	9
2.2 Energy metabolism in the healthy brain	10
2.2.1 Aerobic and anaerobic energy production.....	11
2.2.2 Glucose uptake and differences in glycolysis between neurons and astrocytes	12
2.2.3 Lactate and the astrocyte-neuron lactate shuttle (ANLS) theory..	14
2.2.4 Pentose phosphate pathway and reduction-oxidation balance	17
2.3 Brain energy metabolism and oxidative stress in schizophrenia	18
2.3.1 Glycolysis and ATP regulation	18
2.3.2 Lactate and pH	20
2.3.3 Oxidative stress	21
2.3.4 Summary	22
2.4 Computational modelling of brain energy metabolism.....	23
3.OBJECTIVES	26
4.MATERIALS AND METHODS	27
4.1 Selection and description of the brain energy metabolism model.....	27
4.2 Differential expression analysis.....	31
4.3 Imputation of cell-type specific gene expressions	32
4.4 Brain energy metabolism simulations	33
4.5 On the use of RNA sequencing data.....	35
5.RESULTS	36
5.1 Differentially expressed genes, protein expressions and selection of simulation genes.....	36
5.2 Simulation of altered expression of energy metabolism genes.....	41
5.2.1 Prefrontal cortex (PFC) simulations	43
5.2.2 Anterior cingulate cortex (ACC) simulations	45
6.DISCUSSION.....	46
6.1 Evaluation of materials and methods	46
6.1.1 Winter model.....	46
6.1.2 Limitations of post-mortem bulk RNA sequencing data	47
6.2 Differentially expressed Winter model genes	49
6.2.1 Overview of the differential expression analysis results.....	49

6.2.2	Glycolytic enzymes and phosphotransferases	50
6.3	Effects of altered gene expression on central energy metabolites.....	52
6.3.1	Overview of the brain energy metabolism simulation results	52
6.3.2	PFKM and LDHB	53
6.4	Summary	54
7.	CONCLUSION	56
	REFERENCES.....	57
	APPENDIX 1: BRAIN ENERGY METABOLISM MODELS	67
	APPENDIX 2: THE R CODE	71

LIST OF SYMBOLS AND ABBREVIATIONS

Proteins

AK	Adenylate kinase
CK	Creatine kinase
EAAT	Excitatory amino acid transporter
GLUT	Glucose transporter
GND	Phosphogluconate dehydrogenase
HK	Hexokinase
LDH	Lactate dehydrogenase
MCT	Monocarboxylate transporter
NMDAR	N-methyl-D-aspartate receptor
Nrf2	Nuclear factor-erythroid 2-related factor-2
PDH	Pyruvate dehydrogenase
PDK4	Pyruvate dehydrogenase kinase 4
PFKFB3	6-phosphofructose-2-kinase/fructose-2,6-bisphosphatase-3
PFK	Phosphofructokinase
PGI	Glucose-6-phosphate isomerase
PGK	Phosphoglycerate kinase
PK	Pyruvate kinase
PV	Parvalbumin
RKI	Ribose-5-phosphate isomerase
RPE	Ribulose-phosphate 3-epimerase
SOL	6-phospho-gluconolactonase
TAL	Transaldolase
TKL	Transketolase
ZWF	Glucose-6-phosphate dehydrogenase

Metabolites

ADP	Adenosine diphosphate
Acetyl-CoA	Acetyl coenzyme A
AMP	Adenosine monophosphate
ATP	Adenosine triphosphate
Cr	Creatine
E4P	Erythrose-4-phosphate
F1,6BP	Fructose-1,6-bisphosphate
F2,6BP	Fructose-2,6-bisphosphate
F6P	Fructose-6-phosphate
GABA	Gamma-aminobutyric acid
GAP	Glyceraldehyde-3-phosphate
GLC	Glucose
GLU	Glutamate
GSH	Glutathione
G6L	6-phosphogluconolactone
G6P	Glucose-6-phosphate

LAC	Lactate
NAD(H)	Nicotinamide adenine dinucleotide
NADP(H)	Nicotinamide adenine dinucleotide phosphate
PCr	Phosphocreatine
PEP	Phosphoenolpyruvate
PYR	Pyruvate
P6G	6-phosphogluconate
Ru5P	Ribulose-5-phosphate
R5P	Ribose-5-phosphate
S7P	Sedoheptulose-7-phosphate
X5P	Xylulose-5-phosphate

Other

ACC	Anterior cingulate cortex
ANLS	Astrocyte-neuron lactate shuttle
DE	Differential expression
DLPFC	Dorsolateral prefrontal cortex
E/I	Excitatory/inhibitory
FE	First-episode (schizophrenia)
GWAS	Genome wide association study
HC	Healthy control (sample)
iPSC	Induced pluripotent stem cell
MRS	Magnetic resonance spectroscopy
PET	Positron emission tomography
PFC	Prefrontal cortex
PPP	Pentose phosphate pathway
Redox	Reduction-oxidation
ROS	Reactive oxygen species
SCZ	Schizophrenia (sample)
TCA	Tricarboxylic acid
³¹ P-MRS	Phosphorus magnetic resonance spectroscopy

1. INTRODUCTION

Schizophrenia is a psychiatric disorder which affects around 1 % of the human population [1–3]. It typically develops in early adulthood, and the symptoms of the disorder persist throughout the person's lifetime [1–3]. Although schizophrenia is a common mental disorder which has been studied for decades, its exact causes remain unclear. The aetiology and pathophysiology of the disorder have been connected to various factors including abnormalities in the common neurotransmitters such as dopamine, glutamate and gamma-aminobutyric acid (GABA) [2–5], as well as genetic and environmental factors [2, 6, 7]. In addition, there is an increasing interest in the connection between dysfunction of brain energy metabolism and schizophrenia [8–10].

The brain requires a substantial amount of energy to support signalling activities and maintain ion gradients, especially at excitatory glutamatergic synapses. The focus of this thesis is on neurons and astrocytes, which have complementary energy metabolism profiles: astrocytes rely more on glycolysis, whereas neurons preferentially utilize mitochondrial respiration for energy production. In addition, it has been hypothesized that in response to synaptic transmission, astrocytes increase their glycolytic activity to produce lactate, which is then transported to neurons for mitochondrial energy production. These bioenergetic processes are tightly regulated to ensure adequate energy supply for synaptic activity. [11–13] Accumulating evidence now suggests that several energy metabolism processes are disrupted in the schizophrenic brain, potentially impacting synaptic function and neuronal health [8–10]. However, more information is still needed on how specific genetic and molecular components contribute to the energy metabolism dysfunction in schizophrenia. One effective method for studying the complex processes of brain energy metabolism is computational modelling, which enables the investigation of different molecular components both individually and collectively.

First, post-mortem RNA sequencing data was used to perform differential expression (DE) analysis to study how the expression of cytosolic energy metabolism genes is altered in schizophrenia patients vs healthy individuals. Next, the effects of gene expression alterations were simulated by using computational modelling of brain energy metabolism. The aim of the simulations was to study how the gene expression changes influence the concentrations of central energy metabolites. However, only the effects of

cytosolic genes could be studied, because most computational models do not depict mitochondrial energy metabolism processes in detail. Nonetheless, combining DE analysis with brain energy metabolism simulations provides new information on the impact of schizophrenia-related gene expression changes on cytosolic bioenergetics in schizophrenia.

2. LITERATURE REVIEW

2.1 Schizophrenia

Schizophrenia is a mental disorder which has a lifetime prevalence of approximately 1 % worldwide [1–3]. The symptoms of the disorder are typically divided into three categories: positive, negative and cognitive. Common positive symptoms include hallucinations and delusions, whereas the negative symptoms include lack of pleasure, social withdrawal and diminished ability to initiate and follow through on plans [1, 2, 6]. Furthermore, it has been estimated that two-thirds of schizophrenia patients also experience cognitive impairments [14]. These impairments include problems in attention and concentration, learning and memory, and executive functions, such as abstract thinking and problem-solving [1–3]. Schizophrenia develops typically between the ages of 16 and 30 and it lasts throughout the person's lifetime [1]. The negative and cognitive symptoms usually develop several months to years prior to the appearance of the first psychotic episode, and this period of the disorder is called the prodrome [2, 3, 15]. Schizophrenia is a disorder associated with significant financial and societal costs due to social and occupational impairment, as well as reduced life expectancy caused by increased risk of alcohol and drug problems, anxiety, depression and consequently, suicide [1, 3, 7].

Although schizophrenia inflicts great personal and societal burden, researchers have not been able to fully uncover the aetiology of the disorder to this day. The two main hypotheses which have tried to explain schizophrenia aetiology are called neurodevelopmental hypothesis and dopamine hypothesis. The neurodevelopmental hypothesis postulates that the pathophysiology of schizophrenia is linked to abnormal early brain development, and especially to problems in synapse formation and connectivity [1, 4, 6, 7, 16]. On the other hand, the dopamine hypothesis suggests that dysregulation of synthesis and release of a neurotransmitter called dopamine is behind the disorder [4, 5, 15]. The problem with these hypotheses is that neither can alone explain the complex mechanisms behind schizophrenia. In addition, other factors such as dysregulation of common neurotransmitters glutamate and gamma-aminobutyric acid (GABA) [2, 3, 15], immunological pathways [7, 17], oxidative stress [18, 19] and energy metabolism dysregulation [8–10, 18] have gained interest in recent years. It is also known that both genetics and environmental risk factors contribute to the pathophysiology of schizophrenia [2, 6, 7, 16]. Thus, based on the current knowledge,

the symptoms of schizophrenia are caused by genetic and environmental factors which together disrupt normal brain development and lead to imbalance of important neurotransmitters. The possible mechanisms behind the pathophysiology of schizophrenia will be discussed in the following chapters.

2.1.1 Genetics and environmental factors

Schizophrenia is recognized as a highly heritable disorder, confirmed by a large number of twin, family and adoption studies [1, 2, 7]. In addition, the introduction of large-scale genome-wide association studies (GWAS) has increased the knowledge on the role of genetics in schizophrenia in recent years [2, 7]. The prevailing hypothesis is that schizophrenia is a polygenic disease in which many common genetic variants with small effect sizes, along with a few rare variants with large effect sizes, together contribute to the pathophysiology of the disorder [2, 4, 7]. Additionally, there are currently more than 100 genetic loci associated with schizophrenia [2, 7]. Pathways which are commonly associated with schizophrenia include for example neuronal signalling and synaptic function, as well as multiple neurotransmitter systems (dopamine, glutamate and GABA) [2–4, 7].

In addition to genetic risk factors, multiple environmental risk factors have been associated with schizophrenia [1, 7, 16]. Some environmental factors affect the prenatal phase whereas others have an impact in childhood and adolescence. The prenatal risk factors include obstetric complications [1, 2, 6, 7], lower birth weight [6, 16] and prenatal infections [1, 6, 7, 16], whereas risk factors in childhood and adolescence include adverse upbringing and psychosocial adversity [6, 7, 16], urban environment [1, 6, 7, 16], migrant status [6, 7, 15] and cannabis use [5, 7, 15]. Although a wide variety of genetic and environmental risk factors of schizophrenia have already been identified, how these factors contribute individually and collectively to the aetiology and pathophysiology of this disorder is still poorly understood.

2.1.2 Dopamine

Dopamine is a neurotransmitter which controls many functions such as cognition, emotion and positive reinforcement [20, 21]. The dopamine hypothesis has been the leading hypothesis for the aetiology of schizophrenia since the 1970s, and it was originally based on two lines of evidence. Firstly, multiple studies showed that drugs that activate the dopamine system, such as amphetamine, can induce psychotic symptoms in healthy volunteers and worsen these symptoms in schizophrenia patients [5, 15, 21].

Secondly, it was discovered that antipsychotic drugs act on blocking the D2/3 dopamine receptors, and the effectiveness of these drugs is directly related to their affinity for the dopamine receptors [5, 15, 21]. To this day, all licensed drugs for treating schizophrenia are D2/3 receptor blockers [3, 5, 22].

In the beginning, the dopamine hypothesis of schizophrenia was based on hyperdopaminergia, meaning that it was thought that there is excessive dopamine activity in the brain [5, 23]. However, in the 1990s this hypothesis was modified based on new evidence from post-mortem, imaging and animal studies [5]. This new version of the hypothesis states that dopaminergic abnormalities in schizophrenia are regional: there is hyperdopaminergia in the striatum but hypodopaminergia in the prefrontal cortex (PFC) [3, 5, 21]. These dopaminergic abnormalities are hypothesized to be presynaptic because of evidence suggesting brain-region specific alterations in dopamine synthesis and release capacity [3, 15]: studies have shown that dopamine synthesis and release capacity is increased in the striatum [3–5], and reduced in the PFC [3, 15]. Lastly, latest meta-analyses have not found significant alterations in D2/3 receptors *in vivo* in the striatum or cortex when comparing schizophrenia patients to healthy controls [3].

This evidence pointing to regional differences in dopamine dysregulation shows why current antipsychotics are not capable of treating schizophrenia efficiently. Firstly, these drugs diminish only the psychotic symptoms but have very little effect on the negative and cognitive symptoms [1, 3, 24]. In addition, in around 20–30 % of patients antipsychotic medications have little to no beneficial effect even on the psychotic symptoms, and intolerable adverse effects are quite common [3, 7]. These shortcomings of current antipsychotics have motivated researchers to look for better drug targets that could help alleviate the negative and cognitive symptoms in addition to the psychotic symptoms. Genetic findings actually indicate that up-stream pathways which control the dopamine systems, particularly those involving glutamatergic systems, could potentially have more effective targets for antipsychotic drugs [15].

2.1.3 Glutamate, GABA and excitatory/inhibitory balance

Although dopamine is the neurotransmitter which has been in the centre of attention for decades, there is also increasing interest in glutamate and GABA in schizophrenia research. Glutamate is the primary excitatory neurotransmitter in the brain, and it has an important role controlling synaptic plasticity [25]. GABA on the other hand is the most

common inhibitory neurotransmitter in the brain [26]. These two neurotransmitters together create tightly controlled excitatory/inhibitory (E/I) balance in the brain, and aberrant function of either neurotransmitter system can cause disruptions to this delicate balance [4]. Recent genome-wide association studies have identified a variety of genes related to both glutamatergic and GABAergic function in schizophrenia, and dysregulation of both of these systems has been investigated in various other studies as well [4].

The interest in glutamate emerged when studies showed that phencyclidine and ketamine could induce not only positive, but also negative and cognitive symptoms in healthy individuals, and worsen these symptoms in schizophrenia patients [24, 27–29]. It was discovered that phencyclidine and ketamine act by non-competitively blocking the N-methyl-D-aspartate receptor (NMDAR) channel. NMDAR is an ionotropic postsynaptic glutamate receptor, and blocking of this receptor thus inhibits glutamatergic neurotransmission [30]. There is evidence on hypofunction of NMDAR in schizophrenia [3, 15, 24] but the cause of this hypofunction is still unclear. Genetic studies have found differences in NMDAR subunit expressions, but the results are conflicting and likely vary between different brain areas and subunits [3, 4]. Lastly, a variety of studies have also investigated the differences in glutamate and GABA concentrations between schizophrenia patients and healthy individuals. Again, the results are variable, and suggest regionally specific concentration changes [28, 29, 31–33]. However, post-mortem studies have been able to show that numerous GABA markers have lower mRNA and/or protein expression in the PFC [3, 4, 32].

It is evident that glutamatergic and GABAergic alterations cause imbalance between excitatory and inhibitory neurotransmission, but what could be the cause of this imbalance? One theory implicates synaptic pruning as a key factor in controlling E/I balance. In early development, synaptic density increases rapidly, which is then followed by synaptic elimination from puberty to early adulthood [2, 4]. The goal of this synaptic pruning is to reduce the number of excitatory synapses which leads to increase in inhibitory activity and reduction in unwanted and uncontrolled excitatory activity [3, 4]. Evidence from post-mortem and *in vivo* imaging studies indicates that there is abnormal synaptic formation and/or pruning in frontal cortical regions in schizophrenia [2–4]. This aberrant pruning is hypothesized to lead to loss of glutamatergic synapses, and thus cause E/I imbalance [2–4]. No studies have assessed *in vivo* synaptic changes of GABA yet, so it is unclear if GABAergic synapses are also involved in aberrant synaptic pruning [3]. Nevertheless, it seems that excitatory/inhibitory imbalance, among other factors

discussed in previous chapters, significantly contributes to the pathophysiology of schizophrenia.

2.1.4 Dysfunction of neural circuits and connection to symptoms

The previous chapters have showcased that genetic and environmental factors together with neurotransmitter abnormalities contribute to the pathophysiology of schizophrenia. Regardless, it has been challenging to uncover how these factors individually and collectively cause the positive, negative and cognitive symptoms of schizophrenia. One of the current hypotheses indicates the fronto-striatal neural circuits as a key element in the pathophysiology of schizophrenia [3].

According to this hypothesis, aberrant pruning of glutamatergic synapses together with environmental and genetic factors leads to excitatory/inhibitory imbalance in the PFC of the schizophrenic brain [3, 4]. In the cortex, there are glutamatergic pyramidal neurons which have an important role in stimulating GABAergic interneurons, which subsequently inhibit and control a subpopulation of glutamatergic neurons projecting to the striatum [3, 34]. It has been hypothesized that fewer glutamatergic synapses together with hypofunction of NMDARs causes reduced stimulation of GABAergic interneurons in schizophrenia. Consequently, GABAergic interneurons then have a reduced capability to inhibit glutamatergic neurons projecting to the striatum. These glutamatergic neurons control striatal dopaminergic neurons, and decreased inhibition of the glutamatergic neurons thus leads to overactivation of striatal dopaminergic neurons. [3, 4, 34] This hypothesis on the aetiology of schizophrenia is summarized in Figure 1.

There are multiple lines of evidence supporting this hypothesis. Firstly, NMDAR blockers like ketamine reduce cortical GABA markers, and increase dopamine levels and synthesis capacity in the striatum [3]. Secondly, a recent study showed that the changes in dopamine levels induced by ketamine can be blocked by activating GABAergic interneurons [35]. These findings together link cortical E/I imbalance to striatal hyperdopaminergia.

Although there is increasing evidence of fronto-striatal dysfunction, it is not fully evident how the dysfunction of this circuit causes the symptoms of schizophrenia. Nonetheless, psychotic symptoms of schizophrenia have been linked to increased dopamine in the striatum [3, 4]. It has been hypothesized that the overactive dopamine system would cause all stimuli independent of their importance to generate a maximal dopamine signal.

This would lead to a situation where it is difficult to separate relevant stimulus from irrelevant one, leading the patient to assign too much importance to stimuli that would otherwise be ignored. [5, 6, 22] Thus, these false associations and misperceptions can result in delusions and hallucinations, respectively [3].

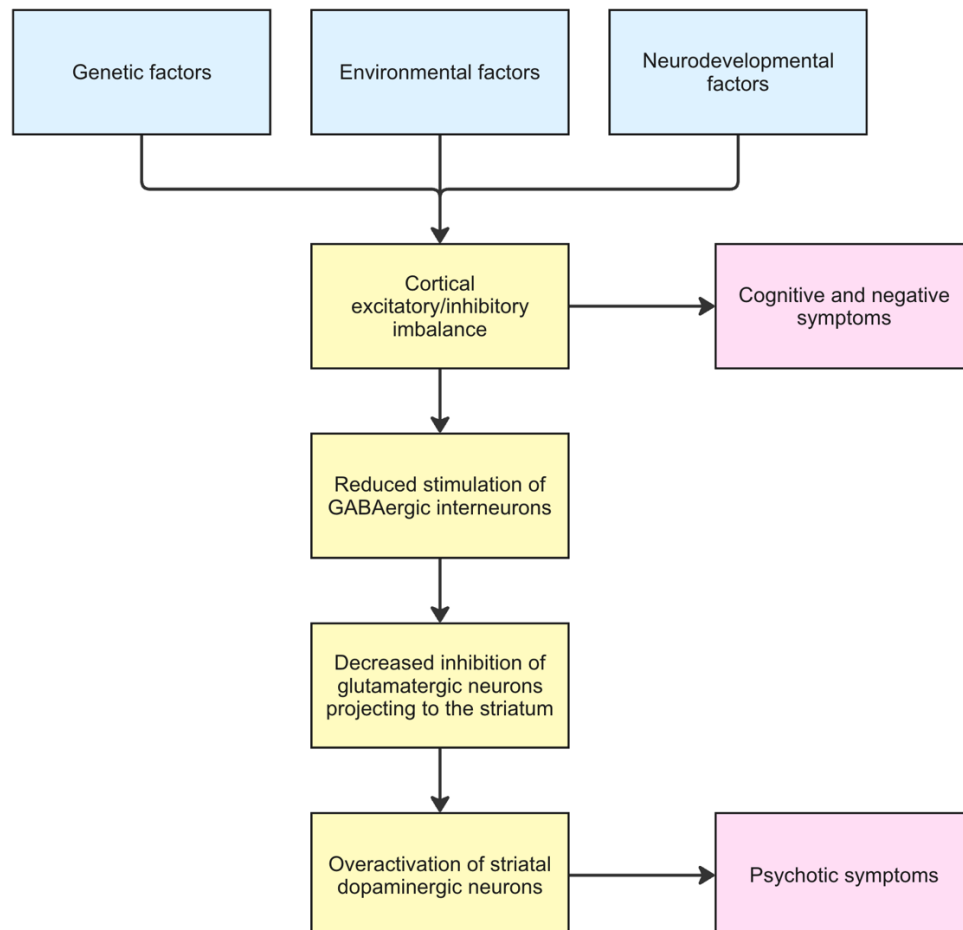


Figure 1. Current hypothesis on the aetiology of schizophrenia. Figure adapted from [4].

Furthermore, the mechanisms underlying the negative and cognitive symptoms of schizophrenia are not well established as of today. One theory proposes that cognitive symptoms result from cortical hypodopaminergia, which impairs prefrontal cortex function, whereas negative symptoms are a result of striatal hyperdopaminergia that disrupts reward signalling [3]. Additionally, hypofunction of anterior cingulate cortex (ACC) has been associated with the negative symptoms of schizophrenia [36, 37]. The ACC is a brain region involved in diverse cognitive and emotional functions such as motivation, memory and attention. One imaging study found a significant inverse relationship with striatal dopamine synthesis and glutamate concentration in the ACC of

first-episode psychosis patients [38]. This finding connects the hypoactivity of the ACC to striatal hyperdopaminergia and the subsequent negative symptoms.

Although considerable advancements have been made in recent years, further research is needed to better understand the temporal, regional and causal relationships between the large variety of factors contributing to schizophrenia. It is also worth mentioning that other brain regions, neurotransmitters and neural circuits are also likely involved in the pathophysiology of schizophrenia. Lastly, it has been shown that there is considerable heterogeneity between schizophrenia patients [3], and in addition, factors such as antipsychotic status and disease progression need to be taken into consideration in research planning, data analysis and interpretation of results.

2.1.5 Astrocytes

While schizophrenia research has traditionally focused on neurons and neuronal circuits, increasing attention is now being directed towards the role of glial cells in schizophrenia pathology. This chapter will focus on astrocytes, but it is worth noting that aberrant function of other glial cells, including microglia and oligodendrocytes, has also been linked to schizophrenia [39, 40]. It is nowadays well known that astrocytes play a crucial role in regulating the formation and maintenance of synapses and the modulation and synchronization of synaptic transmission [39, 41, 42]. Therefore, it is not surprising that astrocyte impairment has been linked to schizophrenia-associated cognitive dysfunction [39, 41].

Firstly, several post-mortem immunohistochemical studies have shown alterations in astrocyte density and aberrant astrocyte morphology in schizophrenia [39–42]. However, there is considerable heterogeneity in the density findings: some studies have reported increased, and other decreased astrocyte density [39–42]. These confounding results are likely explained by use of post-mortem tissue, differences in brain regions and medication status [41, 42]. Nonetheless, multiple animal studies have shown that changes in astrocytic density and morphology in the PFC result in cognitive impairments such as deficits in attention, memory and learning in rodents [43, 44].

It has been hypothesized that the problems in morphological and functional maturation of astrocytes are caused by impairments in their proliferation, differentiation and maturation [39, 41]. Genetic studies have discovered that schizophrenia risk loci are enriched in genes related to astrocyte differentiation and maturation [41]. In addition,

many genes regulating astrocyte proliferation are downregulated during postnatal astrocyte maturation in schizophrenia [41]. Failures in astrocyte maturation and differentiation have been shown to lead to excessive elimination of synapses, disturbances in neurotransmitter systems and aberrant synaptic transmission [39, 42].

Lastly, astrocytes have been associated with dysregulation of glutamatergic pathways related to schizophrenia [39–42]. Post-mortem studies have identified reduced expression of astrocytic glutamate transporters (EAAT1 and EAAT2), glutamine synthetase, glutamate dehydrogenase and glutaminase in schizophrenia [39, 41]. In addition, a few animal studies have demonstrated that genetically induced loss of EAAT1 and EAAT2 causes behavioural phenotypes associated with schizophrenia [42]. Glutamatergic dysfunction has also been associated with reduced D-serine in the schizophrenic brain [39–42]. D-serine is an important amino acid released by astrocytes, and it is needed alongside glutamate to activate postsynaptic NMDA receptors. Mutations in D-serine metabolizing enzymes have been identified as risk factors for schizophrenia [40], and in addition, there is evidence of excessive D-serine degradation in schizophrenia [41]. These disturbances in D-serine metabolism have been hypothesized to cause hypofunction of NMDA receptors, and consequently impaired synapse formation and synaptic plasticity [41]. Finally, there is an indication that altered gene and protein expression of astrocytes could also be linked to the dopaminergic dysfunction seen in schizophrenia [40, 41].

2.2 Energy metabolism in the healthy brain

The brain is an organ which requires disproportional amount of energy in comparison to its weight: it corresponds to only two per cent of the total body mass but around 20 % of the oxygen and 20–25 % of the glucose consumed by the human body are used for brain functions [11, 12, 45, 46]. The high energy need is accounted for primarily by signalling activities such as maintenance and restoration of ion gradients and uptake and recycling of neurotransmitters [11–13, 45]. In addition, synaptic potentials, rather than action potentials, appear to be primarily responsible for the high energetic cost associated with maintaining excitability [13, 45, 47]. In the cerebral cortical gray matter, around 75 % of the energy is used for signalling activities and the remaining 25 % is for non-signalling, basic cellular activities [48]. Out of the signaling activities (75 %), 44 % of the energy is used for synaptic processes (37 % for postsynaptic receptors, ~4 % for presynaptic activities and ~3 % for glutamate cycling), 16 % for action potentials and 15 % for resting potentials.

There are also large differences in energy consumption between cell types: excitatory neurons are responsible for around 80–85 % of energy use in the brain, whereas inhibitory neurons and glial cells together account for around 15–20 %. [45, 48] To sum it up, energy is needed the most in excitatory neurons where signaling activities and maintenance of ion gradients consume a lot of energy. The following subchapters will provide insight into how the high energy needs are met in the brain, what kind of roles do neurons and astrocytes have in energy production, and how these roles complement each other to ensure efficient energy supply in the brain.

2.2.1 Aerobic and anaerobic energy production

Almost all energy-dependent biochemical reactions require energy in the form of adenosine triphosphate (ATP). The brain can use a few different substrates for ATP production, but glucose is the primary energy substrate in the human brain [12, 13, 45, 48]. Another important energy substrate is ketone bodies which the brain uses during development and starvation [13, 45, 48]. Regardless, this thesis will focus on glucose as the main ATP producing substrate.

ATP can be produced both aerobically (with O_2) and anaerobically (without O_2). The anaerobic pathway for ATP production is called glycolysis, and in this pathway, glucose is partially oxidized into two pyruvate molecules. This process takes place in the cytosol and its net yield is two ATP molecules per glucose. In addition, two molecules of a coenzyme called nicotinamide adenine dinucleotide (NAD) are reduced to NADH per one glucose molecule. After glycolysis, pyruvate has two fates: it can be reduced to lactate (anaerobic reaction), or it can be transported into a mitochondrion to continue ATP production aerobically. This aerobic process consists of tricarboxylic acid (TCA) cycle and oxidative phosphorylation, both of which take place in mitochondria. Aerobic ATP production requires O_2 and produces CO_2 and H_2O . Once pyruvate has been transported into a mitochondrion, it is converted into acetyl coenzyme A (acetyl-CoA) which can enter the TCA cycle. The TCA cycle completes glucose oxidation and produces reduced coenzymes and CO_2 . The coenzymes provide electrons for oxidative phosphorylation where the movement of electrons along an electron transport chain creates the energy needed for ATP production. At the end of the electron transport chain, O_2 receives the electrons and H_2O is formed. TCA cycle and oxidative phosphorylation together yield 30–34 ATP molecules per one glucose molecule. [45, 48, 49]

Evidently, aerobic processing of glucose in the mitochondria produces significantly more ATP than anaerobic glycolysis in the cytosol. Therefore, it is not surprising that almost all glucose in the brain is fully oxidized to CO₂ and H₂O in the mitochondria [48, 49]. Nonetheless, glycolysis has an important role in energy production because it can produce energy fast and without the need for oxygen. This quality of glycolysis is especially important during neuronal activity when energy demand increases [13, 45, 48]. Both neurons and astrocytes can metabolize glucose through glycolysis, but they differ in their ability to regulate this process [45, 48]. The next chapter will discuss the differences between neuronal and astrocytic glycolysis in detail.

2.2.2 Glucose uptake and differences in glycolysis between neurons and astrocytes

Before glucose can be used for ATP production it needs to be transported from the bloodstream into the cells. Even though the brain has a high energy demand, it contains very little energy reserves and therefore relies on constant supply of glucose and other energy substrates from the blood circulation [12, 45]. Glucose is transported from the endothelial membrane of the artery to the brain cells through glucose transporters called GLUTs [48]. Endothelial cells and astrocytes express predominantly GLUT1 isoform whereas neurons express predominantly GLUT3 isoform [48, 50]. The driving force for the uptake into the brain is the lower glucose concentration due to continuous glucose metabolism [48]. Once glucose has entered the cell, it can be transported back to the extracellular fluid, or it can be phosphorylated into glucose-6-phosphate (G6P). G6P is a so called “branch-point” metabolite which can have many different fates: it can continue to the glycolytic pathway, enter the pentose phosphate pathway (PPP), be stored as glycogen, or serve as a precursor for a number of compounds such as certain amino-acids and neurotransmitters [12, 45, 48].

As was mentioned in the previous chapter, neurons and astrocytes differ in their ability to regulate glycolysis, and this is due to differences in the expression and regulation of glycolytic enzymes [13, 45, 51]. At the beginning of the glycolytic pathway, G6P is converted to fructose-6-phosphate (F6P) by glucose-6-phosphate isomerase. F6P is a substrate for a key regulatory enzyme of glycolysis, phosphofructokinase-1 (PFK1), which catalyzes the phosphorylation of F6P to fructose-1,6-bisphosphate (F1,6BP) [12, 13, 48]. PFK1 is allosterically activated by fructose-2,6-bisphosphate (F2,6BP) which in turn is synthesized by the 6-phosphofructose-2-kinase/fructose-2,6-bisphosphatase-3 (PFKFB3) enzyme [12, 13, 48]. In neurons, PFKFB3 is continuously degraded by the

ubiquitin-proteasome pathway whereas in astrocytes the expression and activity of this enzyme are high [11–13, 51]. This feature causes neurons to have a slower glycolytic rate since PFK1 cannot be allosterically activated via PFKFB3 and F2,6BP. In addition, there is evidence that astrocytes can activate PFKFB3 by phosphorylation upon cellular energy stress which gives them an important ability to upregulate glycolysis when the energy demand is high [11, 12]. In contrast, one *in vitro* study found out that upregulation of neuronal glycolysis via overexpression of PFKFB3 leads to oxidative stress and apoptosis in neurons [52]. This suggests that the reason why neurons have slower glycolytic rate compared to astrocytes is to protect them from oxidative stress.

Another important energy metabolism enzyme is pyruvate dehydrogenase (PDH) which catalyzes the conversion of pyruvate to acetyl-CoA and thus provides a link between glycolysis and TCA cycle [13, 45, 51]. PDH is inactivated by phosphorylation in astrocytes but not in neurons [45, 49, 51]. PDH is phosphorylated by pyruvate dehydrogenase kinase 4 (PDK4), and the expression of this gene is high in astrocytes compared to neurons [51]. This feature causes astrocytes to rely more on glycolysis for energy producing purposes, and therefore pyruvate is more preferentially converted to lactate instead of acetyl-CoA in astrocytes [13, 45, 51]. The enzyme which catalyzes reduction of pyruvate to lactate is called lactate dehydrogenase (LDH). Neurons and astrocytes express different isoforms of LDH: neurons express only LDH1 (encoded by LDHA gene) [53], whereas astrocytes express both LDH1 and LDH5 (encoded by LDHB gene) [53, 54]. The LDH1 isoenzyme preferentially converts lactate to pyruvate, and LDH5 pyruvate to lactate [53]. Lastly, neurons and astrocytes also express different isoforms of pyruvate kinase (PK) which promotes the conversion of phosphoenolpyruvate to pyruvate: neurons express exclusively an isoform called PKM1 and astrocytes an isoform called PKM2 [51]. To provide some context, PKM2 is typically expressed by proliferating cells as well as cancer cells whereas PKM1 is the dominating isoform in most differentiated adult tissues [55]. The differences in glycolysis and its regulation between neurons and astrocytes are summarized in Figure 2.

To sum it up, the enzymatic profiles of neurons and astrocytes give both cell types their unique properties when it comes to glycolysis and its regulation. Astrocytes can sustain a high glycolytic rate and upregulate the glycolytic flux when energy demand is high. Neurons on the other hand cannot sustain a high glycolytic rate and therefore rely more on aerobic processes of the mitochondria to produce ATP. Nevertheless, it is well known that neurons require significantly more energy than astrocytes, so why do astrocytes have the ability to increase glycolytic rate instead of neurons? There is a theory which

proposes that energy production of neurons and astrocytes is tightly coupled, and that this coupling is mediated through lactate. The next chapter will give an overview of this theory and the evidence both supporting and questioning it.

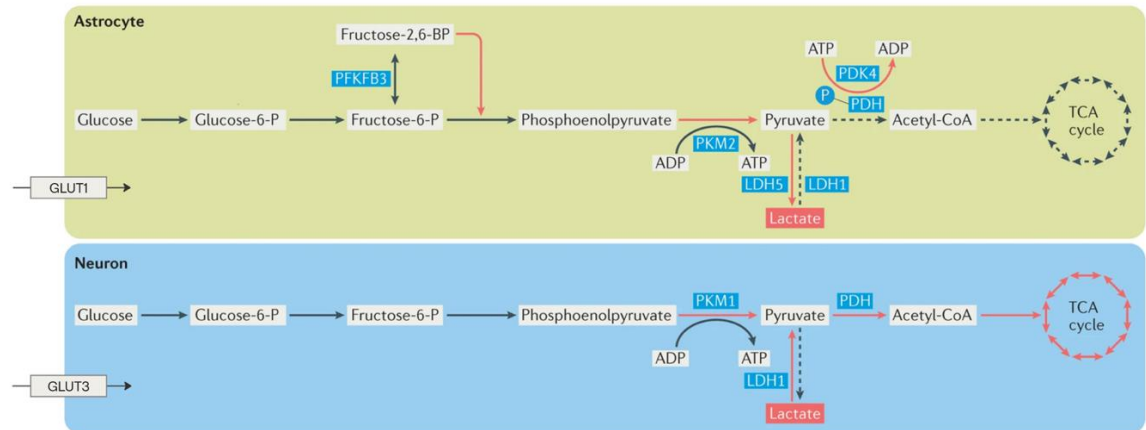


Figure 2. Different glycolytic profiles of neurons and astrocytes. Figure modified from [49].

2.2.3 Lactate and the astrocyte-neuron lactate shuttle (ANLS) theory

For a long time after its discovery in 1780, lactate was thought to be a metabolic waste product which does not have a role in bioenergetics [49, 56–58]. However, after centuries of research lactate has finally begun to be recognized as an important energy source in the brain [45, 49, 56, 57]. In basal conditions, around 10 % of the brain's energy needs are met by oxidation of lactate [59, 60], and this portion can increase under physical activity due to an increase of lactate in the blood circulation [45, 48, 56]. Although lactate's contribution to energy production is relatively small, there are studies showing that the brain preferentially uses lactate as an energy substrate over glucose [45, 49, 56].

Lactate is produced in a metabolic process called aerobic glycolysis which means production of lactate under normal oxygen tension [48, 49]. Aerobic glycolysis occurs in the resting brain, and it increases locally with elevated neuronal activity [59]. In the adult human brain, aerobic glycolysis is concentrated in specific regions [13, 59]: medial and lateral parietal and prefrontal cortices show significant elevations, whereas the cerebellum and medial temporal lobes have significantly lower levels of aerobic glycolysis in comparison to the brain mean value [59]. Lactate is predominantly produced by astrocytes due to their unique enzyme expression profile, which includes expression of lactate dehydrogenase LDH5 and inactivation of pyruvate dehydrogenase [13, 45, 49].

Although astrocytes are the major lactate producers, there is accumulating evidence that the major consumers of lactate are not astrocytes themselves, but neurons instead.

In 1994 Pierre Magistretti and Luc Pellerin published an article which formed the base for a theory called astrocyte-neuron lactate shuttle (ANLS) [61]. This theory postulates that (1) glutamatergic activity increases astrocytic glutamate uptake via excitatory amino acid transporters (EAATs) which co-transport three Na^+ -ions with every glutamate molecule. (2) Increase in intracellular Na^+ concentration activates Na^+/K^+ ATPase which increases ATP consumption, glucose uptake and aerobic glycolysis in astrocytes. (3) Aerobic glycolysis leads to a large increase of lactate which is released to the extracellular space through monocarboxylate transporters (MCT1 and MCT4 in astrocytes). (4) Lactate is taken up by neurons via neuronal lactate transporter (MCT2), and then it is converted to pyruvate and oxidized in mitochondria to produce ATP. [13, 45] These steps of the ANLS theory are presented in Figure 3.

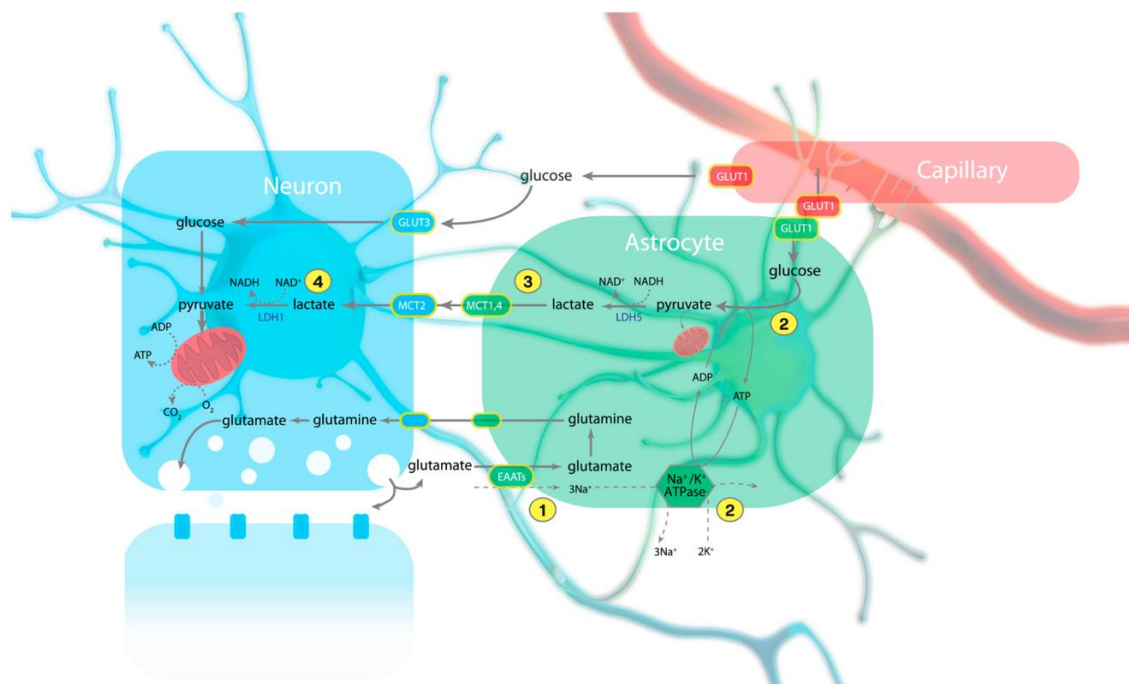


Figure 3. The steps of astrocyte-neuron lactate shuttle. (1) Astrocytic glutamate uptake. (2) Increased Na^+/K^+ ATPase activity, ATP demand and glycolysis in astrocytes. (3) Lactate production and export by astrocytes. (4) Lactate intake, conversion to pyruvate and subsequent mitochondrial processing by neurons. Modified from [13].

Although the ANLS theory has been around for 30 years now, this theory and its details are still a subject of debate (see for example [62] and [63]). Nonetheless, this theory has been gathering more supporters and experimental evidence as time has gone by. Firstly,

multiple studies have shown that the amount of glucose astrocytes take up is disproportionately high compared to their energy demands; it has been estimated that at rest, astrocytes take up at least the same amount of glucose as neurons [45, 49]. In addition, in response to neuronal activity, the majority of glucose uptake occurs in astrocytes [45, 49]. The importance of astrocytic glucose uptake has also been shown in experiments using transgenic mice presenting a haploinsufficiency (only one functional copy of the gene) of glucose transporters [13]. These experiments demonstrated that haploinsufficiency of neuronal GLUT3 did not result in a pathological phenotype or affect glucose utilization, whereas haploinsufficiency of astrocytic GLUT1 lead to severe neurological phenotype. There is also evidence that reduced expression of astrocytic glutamate transporters greatly impairs glucose uptake into astrocytes during functional activation [45, 49]. These studies collectively imply that astrocytic glucose uptake and utilization is dependent on glutamatergic activity and play a crucial role in maintaining proper brain function.

In addition to glucose uptake, multiple studies of both human and rodent brain have showed a transient decrease in extracellular lactate levels after stimulation which is followed by a sustained increase [45]. These results imply that after neuronal activity extracellular lactate is rapidly taken up and oxidized by neurons to meet their immediate energy needs, and the subsequent rise in lactate concentration is caused by sustained astrocytic aerobic glycolysis which replenishes the extracellular lactate pool [13, 45]. Furthermore, at least one study has been able to detect a lactate gradient from astrocytes to neurons *in vivo* [64].

Although a large variety of studies has provided support for the ANLS theory, it has also faced some criticism. First of all, the glutamate induced glucose uptake and lactate release in cultured astrocytes is a phenomenon which some laboratories have been able to replicate but others have not [48, 62]. Secondly, there is also a controversy surrounding how neurons regulate their glycolysis: some studies have showed that neurons possess the ability to upregulate glycolysis [48], while others suggest that neurons have a limited or even no capacity to do so [13]. Additionally, the limitations and differences of the research methods cause significant variability to the results which further complicates the interpretation of the results.

Lastly, it is essential to note that ANLS likely does not operate at all synapses and in all brain regions in an equal manner [49]. Furthermore, the ANLS theory does not discount glucose utilization by glycolysis in neurons (in particular under basal conditions) or TCA

cycle and oxidative phosphorylation in astrocytes [45, 49]. Nevertheless, the ANLS offers an intriguing theory that illustrates how the energy metabolism profiles of neurons and astrocytes complement each other, and how they are linked to glutamatergic activity.

2.2.4 Pentose phosphate pathway and reduction-oxidation balance

In addition to glycolysis, glucose can be processed in a metabolic pathway called the pentose phosphate pathway (PPP) [12, 45, 48]. This pathway utilizes G6P to produce pentoses and ribose-5-phosphate, which can be used for nucleotide synthesis [48]. PPP also generates nicotinamide adenine dinucleotide phosphate (NADPH) which is an important coenzyme for managing cellular reduction-oxidation (redox) state [12, 13, 48]. NADPH serves as an electron donor in a reaction that reduces oxidized glutathione back to its active form, glutathione (GSH) [11–13]. GSH is an electron donor in many redox reactions including detoxification of reactive oxygen species (ROS) [13, 45]. Therefore, constant NADPH supply by PPP maintains the redox balance of the cell and protects it from oxidative stress [11–13].

Since neurons have a high oxidative activity, they have higher basal PPP activity and higher NADPH levels than astrocytes [45, 48]. Despite the high oxidative activity, neurons have a relatively weak antioxidant machinery [11, 65]. In neurons, a master antioxidant transcriptional activator, nuclear factor-erythroid 2-related factor-2 (Nrf2), is constantly destabilized [11, 12]. This protein induces for example the transcription GSH, and the lack of Nrf2 in neurons means that they cannot synthesize GSH *de novo*. On the contrary, Nrf2 is highly stable in astrocytes, so they can synthesize GSH [11, 12]. In addition, astrocytes release GSH precursors which neurons can uptake and use for GSH synthesis [11]. There is also some evidence that GSH precursor release happens in response to glutamatergic activity [65].

In conclusion, neurons must maintain a fine balance between glycolysis and PPP so they can meet their energy needs and maintain their antioxidant potential. Astrocytes also play an important role in helping neurons to maintain this balance: in addition to providing GSH precursors, lactate shuttling between these two cell types can help neurons to produce high amounts of ATP while sparing glucose for PPP [13, 45]. These mechanisms create yet another link between neurons and astrocytes and provide an important way to balance the redox statuses of these cells.

2.3 Brain energy metabolism and oxidative stress in schizophrenia

The pathophysiology of schizophrenia is increasingly associated with disruptions in brain energy metabolism [8–10, 18, 66]. Additionally, increased oxidative stress and alterations in redox balance, which are tightly linked with energy metabolism, have been implicated in schizophrenia [18, 67, 68]. There is evidence of abnormal brain energetics from transcriptomic and proteomic analyses, post-mortem and animal studies, as well as from imaging studies. Since brain energy metabolism is tightly linked with synaptic activity, it has been hypothesized that problems in brain bioenergetics may cause some of the cognitive symptoms of schizophrenia [9, 10]. In recent years, the effects of antipsychotics on metabolic disturbance have been studied increasingly, and now there is substantial evidence indicating that antipsychotics affect glucose metabolism [10, 69]. Yet, there are also many studies showing dysregulation of glucose metabolism in the early stages of schizophrenia, prior to the administration of antipsychotics [10, 18]. Thus, there is some debate on whether disruption of energy metabolism is a primary cause of schizophrenia, or a result of genetics, synaptic dysfunction or antipsychotic use [9]. Taking into consideration the heterogeneity of schizophrenia, it is likely that a combination of multiple disease factors contributes to the disruption of brain energy metabolism.

In addition, there is heterogeneity in the brain regions and bioenergetic pathways which are affected by brain energy metabolism disruptions. Firstly, a variety of studies strongly indicate that the abnormalities in brain energetics are region-specific, and there may be relatively large differences between brain areas [9, 18, 70, 71]. Secondly, it has been suggested that multiple energy metabolism pathways and processes, such as glycolysis, gluconeogenesis, lactate shuttling and metabolite transportation, are altered in schizophrenia [9, 70]. Although there is also strong evidence on mitochondrial abnormalities in schizophrenia [23, 72, 73], this thesis will focus on disruptions in cytosolic energy metabolism processes, because mitochondrial processes are not commonly depicted in detail in brain energy metabolism models (further discussion on this topic can be found in Chapter 2.4).

2.3.1 Glycolysis and ATP regulation

Multiple strains of evidence point to dysregulation of glycolysis in schizophrenia. There are various proteomic studies showing altered expression of many glycolytic enzymes in multiple brain regions including prefrontal cortex (PFC), dorsolateral prefrontal cortex

(DLPFC), anterior cingulate cortex (ACC), and hippocampus (see studies presented in [9, 70]). Moreover, there are regional variations in the differential expression of glycolytic enzymes across different areas of the brain: there are enzymes which are upregulated in one region but downregulated in another.

On top of the altered expression of glycolytic proteins, studies suggest that in the schizophrenic brain, there is a shift in energy metabolism away from mitochondrial respiration (TCA cycle and oxidative phosphorylation) towards glycolysis [8, 18, 74]. This energetic shift is supported for example by evidence showing that the expression of pyruvate dehydrogenase, which controls pyruvate entry into TCA cycle, is decreased in the PFC in schizophrenia [75]. It appears that the shift towards glycolysis is not influenced by antipsychotics, because it was also observed in post-mortem studies of schizophrenia patients who have never used antipsychotics [75]. Lastly, one study found that the expression of glycolytic enzymes was decreased in post-mortem DLPFC neurons, but not in astrocytes [76]. This observation suggests that neurons may increasingly rely on astrocytic glycolysis and astrocyte-neuron lactate shuttle to meet their energy demands in schizophrenia.

There is also evidence of decreased ATP availability due to disruption of creatine kinase (CK) activity in schizophrenia. There are a few phosphorus magnetic resonance spectroscopy (³¹P-MRS) studies showing that the rate-constant of the forward reaction of CK (transfer of an inorganic phosphate to ADP to form ATP) is decreased in schizophrenia. This decrease was observed both in the frontal lobe of first-episode schizophrenia patients [77] and in the medial PFC of chronic [78, 79] schizophrenia patients. In addition, a decrease in creatine concentration [80] and decreased expression of creatine kinase [81] has been found in the ACC of the schizophrenic brain. These findings together suggest that there may be less ATP available in certain regions of the schizophrenic brain, which can lead to disruptions in neuronal communication and presentation of psychotic symptoms [8, 79]. Lastly, some ³¹P-MRS studies have attempted to measure the levels of phosphocreatine (PCr) which is an important cytosolic energy reserve which can be used to rapidly generate ATP [8]. However, the results on PCr/ATP ratio in schizophrenia are inconsistent, likely due to methodological limitations [8].

2.3.2 Lactate and pH

Various studies suggest that brain lactate concentration is increased in schizophrenia [8, 18, 82], and it is hypothesized that this increase is due to increased glycolysis which leads to abnormally high lactate production [18, 83]. A very recent meta-analysis of 13 studies including both in vivo and post-mortem studies showed that the lactate concentration is significantly higher in the schizophrenic brain compared to control individuals [84]. Out of the 13 studies, 10 showed elevated brain lactate levels and three studies showed slightly decreased levels in schizophrenia. The increased brain lactate levels were present in multiple brain regions, including PFC, DLPFC, ACC, hippocampus and striatum. However, the authors of the meta-analysis also concluded that there is no significant difference in *blood* lactate levels between schizophrenia patients and healthy controls.

Although this meta-analysis found a significant increase in brain lactate, it did not investigate how disease progression or use of antipsychotics may influence these results. In fact, there is some evidence suggesting that elevated lactate levels are specifically a characteristic of chronic schizophrenia. Additionally, increase in lactate concentration has been associated with reduced cognitive functioning and functional capacity in one study [85] and with negative symptoms in another study [82]. In contrast, no difference in lactate levels was observed in FE schizophrenia patients versus healthy controls [86], or among clinical high-risk individuals versus healthy controls [8]. Lastly, although some studies have reported no correlation between brain lactate and antipsychotic use [18], there is also evidence suggesting that lactate levels are influenced by antipsychotic drugs [87]. In summary, there is evidence indicating increased brain lactate levels in chronic schizophrenia, and it is possible that antipsychotics have an impact on this increase.

In addition to increased brain lactate, schizophrenia is also associated with decreased brain pH [8, 18, 87]. The decrease in brain pH is at least partly caused by the increase in lactate levels, but mitochondrial dysfunction and decreased electron transport chain activity may also contribute to the acidification of brain tissue [8, 18, 87]. The decrease in brain pH is quite small but significant: it has been estimated that the pH in the schizophrenic brain is on average 0.2 pH units lower than in the healthy brain, based on both post-mortem and MRS imaging studies [87]. However, there is considerable variability in the results of pH studies, and a considerable number of them do not have sufficient power to detect differences in brain pH [8, 18]. Similarly to lactate, studies have

not found a difference in pH between FE schizophrenia patients and healthy individuals, or first-degree relatives of psychosis patients and healthy individuals [8]. These observations suggest that decreased brain pH is a long-term consequence of disturbed brain energy metabolism, although more research is still needed on this topic. Nevertheless, many neurotransmitter receptors and ion channels are sensitive to pH, and pH alterations can also affect membrane excitability and signalling cascades [87]. Lastly, when it comes to schizophrenia, decrease in pH has been shown to increase synaptic dopamine levels, and decrease NMDA receptor activity in rodent models [87]. These studies thus link disrupted bioenergetics and decreased pH to dopaminergic and glutamatergic dysfunction of schizophrenia.

2.3.3 Oxidative stress

Increased oxidative stress in schizophrenia has been implicated in a variety of different studies [18, 23, 68, 88]. The oxidative stress is suggested to be linked to mitochondria: dysregulation of mitochondrial electron transport complexes causes oxidative stress, but in addition, abnormally high generation of reactive oxygen species (ROS) causes mitochondrial damage through oxidation of mitochondrial lipids, sulfhydryl groups, and mitochondrial respiratory enzymes [23, 68, 88]. Besides mitochondria, other factors which have an important role in regulating the redox balance and protecting the cells from oxidative stress have been shown to be impaired in schizophrenia.

Disruptions of many different components of the antioxidant defense system have been observed in the schizophrenic brain (see for example table 1 in [89]). Firstly, there is evidence from ^{31}P -MRS studies showing that the ratio of an important redox pair, NAD/NADH, is reduced in schizophrenia. One study found a significant reduction of NAD/NADH ratio in the frontal cortex of FE psychosis patients relative to controls [90], while another study found a significant NAD/NADH ratio reduction in both FE and chronic schizophrenia patients relative to healthy individuals [67]. Furthermore, it was discovered that the NAD/NADH ratio was 15 % lower in FE schizophrenia patients compared to chronic patients [67].

Another molecule implicated in oxidative stress in schizophrenia is the key antioxidant glutathione (GSH). Multiple post-mortem studies have shown that GSH levels are decreased in the PFC as well as in the cerebrospinal fluid and peripheral tissues in schizophrenia [88, 91]. Although *in vivo* studies of GSH levels have provided inconsistent results [8, 88], two meta-analyses of MRS studies found a significant decrease of GSH

in the ACC of the schizophrenic brain [92, 93], and yet another study found a negative correlation between GSH levels in the posterior medial PFC and the severity of negative symptoms in schizophrenia patients [94]. However, further research on GSH levels is needed, particularly to account for antipsychotic use and disease status (FE or chronic).

2.3.4 Summary

The previous chapters presented some key evidence indicating dysregulation of cytosolic energy metabolism and redox balance in schizophrenia, summarized in Figure 4. Based on current knowledge, it seems like first-episode schizophrenia is characterized by redox dysregulation and mitochondrial dysfunction. This early phase of the disorder is associated with reduced ATP availability due to decreased CK reaction rate and possibly PCr/ATP ratio, and redox imbalance caused by decreased NAD/NADH ratio. The changes in redox balance can subsequently lead to NMDAR hypofunction, which causes excitatory/inhibitory imbalance, leading to some cognitive symptoms of schizophrenia. In addition, NMDAR hypofunction can alter the transcription control of antioxidant genes, leading to further oxidative stress and NMDAR hypofunction. [8]

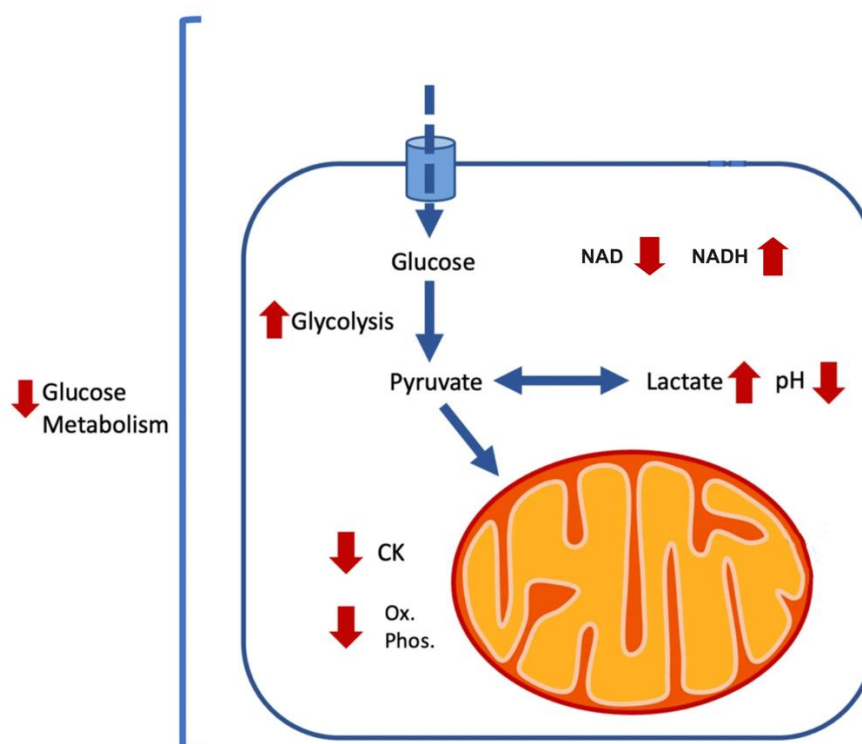


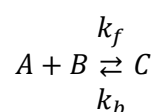
Figure 4. Summary of changes in energy metabolism and redox balance in schizophrenia. Oxidative phosphorylation (ox. phos.), forward reaction rate of creatine kinase (CK). Modified from [8].

It has been hypothesized that the schizophrenic brain attempts to restore the redox balance and return ATP availability to normal by shifting from oxidative phosphorylation towards glycolysis. This shift helps diminish the production of ROS via oxidative phosphorylation but ensures ATP production through glycolysis. The result of this shift is increased lactate concentration and a subsequent decrease in pH in the schizophrenic brain. [8]

2.4 Computational modelling of brain energy metabolism

A wide variety of computational models have been developed over the years to describe numerous brain functions, including energy metabolism. Although different approaches have been used to depict metabolic pathways of the brain over multiple decades, this chapter will focus on brain energy metabolism models which combine energy metabolism with neuronal activity and hemodynamics. These kinds of models enable the study of changes in energy metabolism reactions in response to neuronal activity over a specified time period. Since the energy consumption and production of the brain are tightly linked to changes in neuronal activity, these models can help provide detailed information on brain energetics. The first model to combine neuronal activity, brain energy metabolism and hemodynamics is by Aubert et al. from 2001 [95]. Since then, Aubert and colleagues as well as other researchers in the field have refined this model and also developed new brain energy metabolism models by introducing alternative modelling approaches.

The vast majority of brain energy metabolism models are so called multi-compartment models [96]. The compartments typically represent cells, blood vessels, extracellular space or even smaller compartments like organelles. Each compartment consists of a set of specified biomolecules and the reactions between them. It is assumed that a compartment is well mixed, meaning that (1) every biomolecule can react with any other biomolecule in the same compartment if the reaction is thermodynamically and enzymatically possible, and (2) the reactions happen without a delay due to diffusion or translocation. [96] Furthermore, it is assumed that the law of mass action is in effect, according to which the rate of a chemical reaction is proportional to the product of the concentrations of the reactants [97]. For example, given a chemical reaction



the rate of the reaction is given as

$$v = A \times B \times k_f - C \times k_b$$

where k_f and k_b are the rate constants [97, 98]. This means that the rate of concentration change of species A and B is

$$\frac{d[A]}{dt} = \frac{d[B]}{dt} = -k_f[A][B] + k_b[C]$$

and the rate of concentration change of species C is

$$\frac{d[C]}{dt} = -k_b[C] + k_f[A][B]$$

Lastly, most brain energy metabolism models are deterministic and governed by systems of coupled ordinary differential equations representing enzymatic and transport reactions of metabolites [96].

Although most brain energy metabolism models are multi-compartmental, assume the compartments are well mixed and apply the law of mass action, there are also considerable differences between the models. One major difference is the modelling of lactate transfer between neurons and astrocytes. As was discussed in Chapter 2.2.3, the ANLS theory is supported by many researchers but objected to by others, and this divide also exists in the brain energy metabolism modelling. Some models are in accordance with ANLS theory, but others inversely predict that lactate is produced by neurons and taken up by astrocytes. The conflicting approaches to lactate transport appear to stem from different interpretations on glucose uptake and glycolytic activity in response to activation in neurons and astrocytes [96, 99, 100]. Models supporting ANLS cite studies indicating that astrocytes are primarily responsible for glucose uptake during neuronal activation, as well as studies suggesting that neurons cannot significantly upregulate their glycolytic activity in response to activation [99]. On the other hand, models which support lactate transfer from neurons to astrocytes refer to studies implicating increased glucose uptake and glycolysis in neurons in response to neuronal activity [100]. These opposing approaches highlight that the brain energy metabolism processes can be modelled in a variety of different ways.

Nowadays, there are multiple computational models of brain energy metabolism, as reviewed in Appendix 1. Although these models share some core features, the level of detail in them varies significantly. In the simplest models, energy metabolism is summarized in only three metabolic reactions involving glucose and lactate (see models presented in [96]). On the other hand, the more complex models can consist of dozens of enzymatic energy metabolism reactions [96]. In addition, there is a lot of variation on which energy-metabolism-adjacent processes, such as glutamate recycling or ion homeostasis, are included in the models [96]. Lastly, most brain energy metabolism models do not contain detailed description of mitochondrial respiration including TCA cycle, oxidative phosphorylation and mitochondrial transport reactions [96]. Thus, the majority of the models are limited to studying only cytosolic energy metabolism processes. Despite this limitation, computational modelling of brain energy metabolism has several benefits: it helps understand and interpret *in vitro* and imaging data and allows detailed inspection of complex metabolic pathways. Finally, modelling can be used for testing hypotheses and predicting outcomes on how genetic disturbances influence brain energy metabolism.

3. OBJECTIVES

The overarching aim of this thesis is to study the energy metabolism of prefrontal cortex (PFC) and anterior cingulate cortex (ACC) in schizophrenia. The first goal of the thesis is to study how the expression of the cytosolic energy metabolism genes is changed in schizophrenia, based on differential expression (DE) analysis. The second goal is to simulate how the changes in gene expression alter the concentrations of central energy metabolites by using brain energy metabolism modelling. Through these endeavors, the ultimate aim of this thesis is to increase knowledge on which genes, proteins and/or biological processes contribute to the brain energy metabolism disruptions associated with schizophrenia.

4. MATERIALS AND METHODS

4.1 Selection and description of the brain energy metabolism model

In order to model how the brain energy metabolism may be altered in schizophrenia, a literature search was conducted to find a suitable biophysically detailed mathematical model depicting brain energy metabolism. The goal was to find a model which portrays specific metabolic and transport reactions which can be modified to represent the energy metabolism processes in the schizophrenic brain. In addition, the goal was to find a study which describes the model in detail and includes all the necessary files and information to replicate the brain energy simulations. Several potential brain energy metabolism models were found, but only some of them were suitable for the purposes of this thesis. The models and their details are presented in Appendix 1.

After thorough analysis and consideration, the model chosen for implementation is a brain energy metabolism model by Winter and colleagues, published in 2018 [101]. The Winter model combines three earlier brain energy metabolism models which are described in Appendix 1. Although Winter et al. investigate Alzheimer's disease in their study, the default model depicts energy metabolism in the healthy brain. The Winter model is a biophysical model which combines brain energy metabolism, neuronal activity and the hemodynamic response together to better understand how the energy metabolism mechanisms respond to a stimulus. In the Winter model, the stimulus is described as a combination of (a) release of glutamate from neurons into the extracellular space coupled with an influx of Na^+ from the extracellular space to the neurons, and (b) an increase in the cerebral blood flow. Lastly, the Winter model supports the ANLS theory.

The Winter model consists of six compartments: neuron, astrocyte, extracellular space, capillary, artery and vein. The metabolic reactions take place in neurons and astrocytes, and the transport reactions occur between the first five compartments. In the model, two central metabolic pathways, glycolysis and PPP, are depicted in detail, whereas TCA cycle and oxidative phosphorylation are represented only by one combined reaction. In total, the Winter model consists of 64 reactions: 40 metabolic reactions and 24 transport reactions. The compartments and transport reactions of the Winter model are presented in Figure 5 and the metabolic reactions are presented in Figure 6.

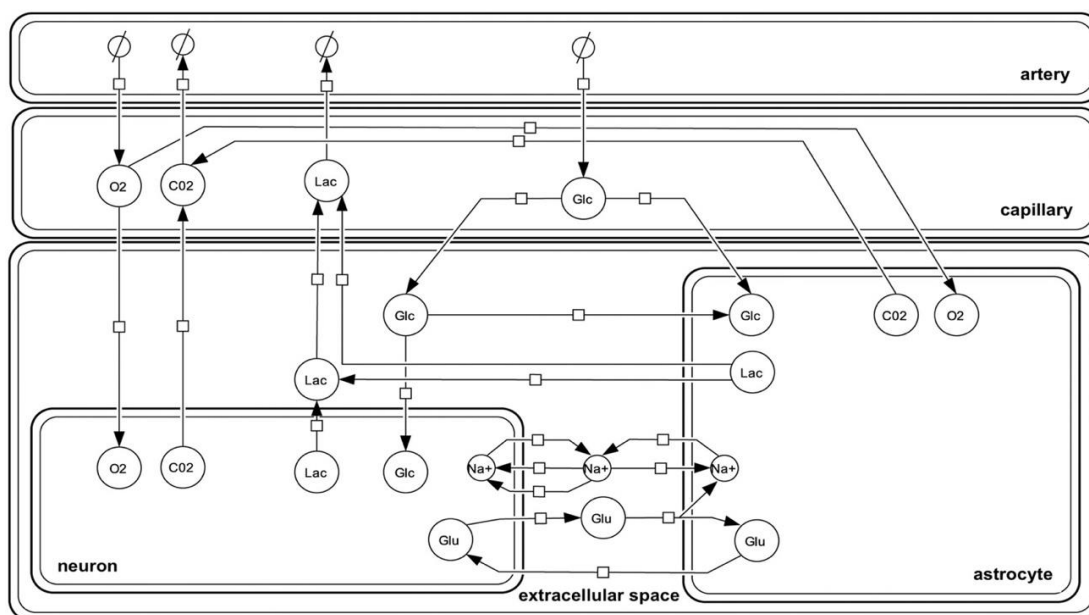


Figure 5. Winter model compartments and transport reactions. All the reactions are reversible. For glucose (GLC), lactate (LAC), oxygen (O₂) and carbon dioxide (CO₂) the arrows indicate the direction of flux at steady state, and for glutamate (GLU) and sodium (Na⁺) the arrows indicate the flux after stimulation. Figure modified from [101].

The proteins involved in the Winter model reactions were specified using the KEGG REACTION Database (<https://www.genome.jp/kegg/reaction/>; 23.8.2024). The KEGG REACTION codes were included in the Winter model, and the protein names and corresponding gene symbols were fetched from the database by using these codes. The gene symbols were obtained for the purpose of the DE analysis (Chapter 4.3). Some reactions did not include the KEGG codes, so those proteins and genes had to be looked up using other databases, primarily UniProt (<https://www.uniprot.org/>; 23.8.2024). The Winter model reactions, proteins and genes are presented in Table 1. Note that the reactions which do not include specific proteins (mitochondrial respiration, O₂ and CO₂ diffusion, and ATP hydrolysis) were not included in the table. Additionally, it is likely that not all the genes listed in Table 1 are expressed by neurons and/or astrocytes. Cell-type specific protein expressions were investigated only for the genes that were determined differentially expressed by the DE analysis (Chapter 4.3).

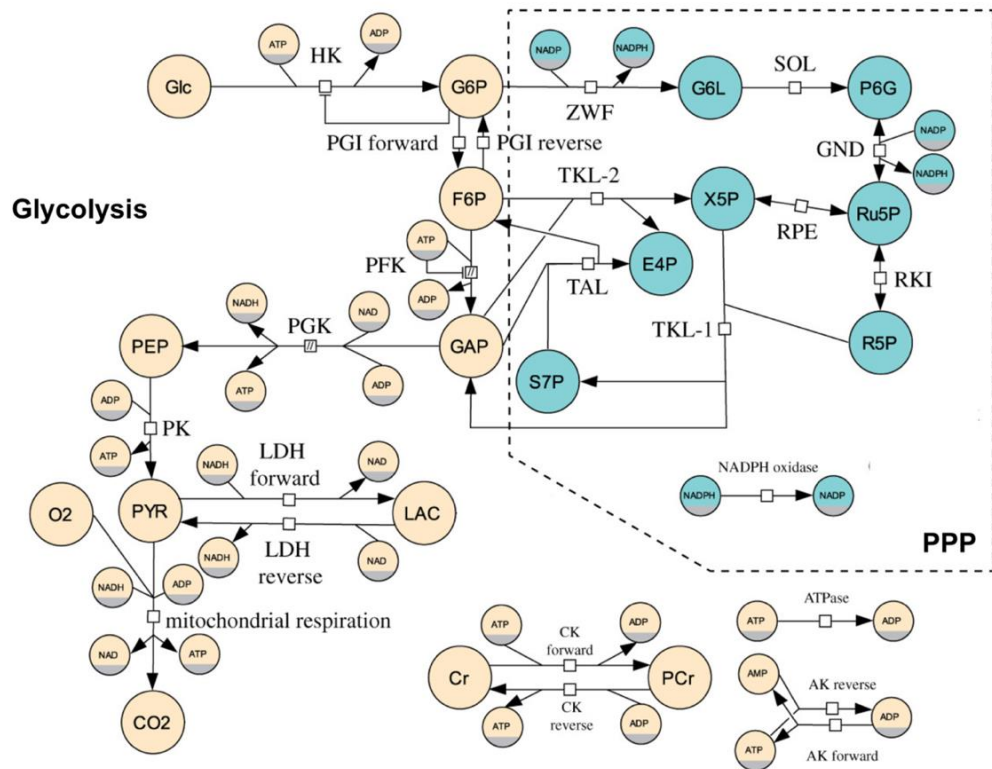


Figure 6. Winter model metabolic reactions. Glycolysis reactions are in yellow and pentose-phosphate pathway (PPP) reactions are in blue inside the dashed lines. Figure modified from [101].

Metabolite abbreviations: glucose (GLC), glucose-6-phosphate (G6P), fructose-6-phosphate (F6P), glyceraldehyde-3-phosphate (GAP), phosphoenolpyruvate (PEP), pyruvate (PYR), lactate (LAC), creatine (Cr), phosphocreatine (PCr), 6-phosphogluconolactone (G6L), 6-phosphogluconate (P6G), ribulose-5-phosphate (Ru5P), ribose-5-phosphate (R5P), xylulose-5-phosphate (X5P), erythrose-4-phosphate (E4P), sedoheptulose-7-phosphate (S7P). Protein name abbreviations: hexokinase (HK), glucose-6-phosphate isomerase (PGI), phosphofruktokinase (PFK), phosphoglycerate kinase (PGK), pyruvate kinase (PK), lactate dehydrogenase (LDH), adenylate kinase (AK), creatine kinase (CK), glucose-6-phosphate dehydrogenase (ZWF), 6-phospho-gluconolactonase (SOL), phosphogluconate dehydrogenase (GND), ribulose-phosphate 3-epimerase (RPE), ribose-5-phosphate isomerase (RKI), transketolase (TKL), transaldolase (TAL).

Table 1. The biochemical reactions and reaction-related proteins of Winter model, as well as the genes encoding the proteins. Metabolite abbreviations can be found from the “List of symbols and abbreviations” section and also from Figure 6 caption above.

Reaction	Protein name(s)	Gene symbol(s)
$ATP + GLC \rightarrow G6P + ADP$	Hexokinase	HK1–3, HKDC1
$G6P \leftrightarrow F6P$	Glucose-6-phosphate isomerase	GPI
$F6P + ATP \rightarrow 2\ GAP + ADP$	1. Phosphofruktokinase-1 2. Fructose-bisphosphate aldolase 3. Triose-phosphate isomerase	1. PFKM, PFKL, PFKP 2. ALDOA, ALDOB, ALDOC 3. TPI1

$GAP + ADP + NAD \rightarrow PEP + ATP + NADH$	1. Glyceraldehyde-3-phosphate dehydrogenase 2. Phosphoglycerate kinase 3. Phosphoglycerate mutase 4. Phosphopyruvate hydratase	1. GAPDH, GAPDHS 2. PGK1, PGK2 3. PGAM1, PGAM2, PGAM4, BPGM 4. ENO1–4
$PEP + ADP \rightarrow PYR + ATP$	Pyruvate kinase	PKLR, PKM
$PYR + NADH \leftrightarrow LAC + NAD$	Lactate dehydrogenase	LDHA, LDHB, LDHC, LDHD
$ATP + 3 Na^+ \rightarrow ADP$	Na ⁺ /K ⁺ -ATPase	ATP1A1–4, ATP1B1–3
$2 ADP \leftrightarrow AMP + ATP$	Adenylate kinase	AK1–9
$PCr + ADP \leftrightarrow Cr + ATP$	Creatine kinase	CKB, CKM, CKMT1A, CKMT1B, CKMT2
$G6P + NADP \rightarrow G6L + NADPH$	Glucose-6-phosphate dehydrogenase	G6PD
$G6L \rightarrow P6G$	6-phospho-gluconolactonase	PGLS, H6PD
$P6G + NADP \leftrightarrow Ru5P + NADPH$	Phosphogluconate dehydrogenase	PGD
$Ru5P \leftrightarrow X5P$	Ribulose-phosphate 3-epimerase	RPE, RPEL1
$Ru5P \leftrightarrow R5P$	Ribose-5-phosphate isomerase	RPIA
$X5P + R5P \rightarrow GAP + S7P$	Transketolase	TKT, TKTL1, TKTL2
$GAP + S7P \leftrightarrow F6P + E4P$	Transaldolase	TALDO1
$NADPH \rightarrow NADP$	NAD(P)H oxidase	DUOX1, DUOX2
<i>GLC transport</i>	Glucose transporters (GLUTs and SGLTs)	SLC2A1–8, SLC5A1–2
<i>LAC transport</i>	Monocarboxylate transporters (MCTs)	SLC16A1–3, SLC16A7–8
<i>GLU transport</i>	Glutamate transporters (EAATs)	SLC1A1–3, SLC1A6–7
<i>Na⁺ leak</i>	Na ⁺ leak channel	NALCN

4.2 Differential expression analysis

The RNA sequencing data used for the differential expression (DE) is from the CommonMind Consortium [102], and it is human post-mortem bulk RNA sequencing data. The CommonMind Consortium database has two data sets corresponding to two brain regions: the prefrontal cortex (PFC) and the anterior cingulate cortex (ACC). The data sets consist of data from both schizophrenia patients (SCZ) and healthy control (HC) individuals. The metadata of the two data sets is presented in Table 2.

The data analysis was performed using R, and the two data sets were analyzed separately. The full R code, the packages used for performing the analyses and their version numbers can be found in Appendix 2. First, the genes whose read count across all samples was in the lowest 10 %, were filtered out to reduce memory use and speed up the analysis. Next, the DE analysis was performed using the *DESeq2* package [103] and its *DESeq* function which uses the Wald test to calculate the statistical significance values. In addition to the pre-filtering, additional filtering of lowly expressed genes was performed by the *results* function of the *DESeq2* package. The *results* function also accounts for multiple testing by using the Benjamini-Hochberg correction. The significance threshold was set at $\alpha = 0.01$.

Table 2. Metadata of the CommonMind Consortium data sets. Note that the number of genes includes both protein-coding and RNA-coding genes.

	Number of subjects	Healthy controls (HC)	Schizophrenia patients (SCZ)	Number of genes
PFC	558	295	263	56,632
ACC	481	251	230	58,929

The design formula used in the analysis was

$$\sim \text{Diagnosis} + \text{Age} + \text{Sex} + \text{PMI} (\text{postmortem interval}).$$

This indicates that, in addition to the diagnosis (SCZ or HC), other factors and their potential variability can be accounted for in the analysis. By adding these factors to the formula, the sensitivity for finding differences which are due to diagnosis status increases.

After the DE analyses of the whole data sets, the genes that are included in the Winter model (see Table 1) were extracted from results. The only gene that was not found from the PFC data set is PGAM2, and the only two genes that were not found from the ACC data set are PGK2 and PGAM2. Lastly, protein expressions of the DE genes were investigated using The Human Protein Atlas (<https://www.proteinatlas.org/>; 27.8.2024) as well as other sources (see Table 6 in Chapter 5.1). Only the genes that had sufficient evidence of protein expression were included in the subsequent analyses.

4.3 Imputation of cell-type specific gene expressions

The RNA-sequencing data used for the DE analysis is bulk data, meaning that the samples consist of a mixture of different cell types from a specific brain region. However, the Winter model has separate reactions for neuronal and astrocytic metabolic processes. Therefore, a tool called CIBERSORTx (<https://cibersortx.stanford.edu>; 27.8.2024) was used to impute cell-type specific gene expressions for neurons and astrocytes from bulk RNA sequencing data.

“Tutorial 5 - Impute Gene Expression, High-Resolution Mode” on the CIBERSORTx website was followed to impute cell-type specific gene expressions. The analysis requires three types of files: signature matrix file, mixture file and gene subset file. Firstly, the signature matrix was constructed based on cell-type specific RNA expression data of the brain, presented in an article by Zhang and colleagues from 2014 [51]. Zhang et al. used adult human cortical brain tissue, purified the cell types (neurons, astrocytes, oligodendrocytes, microglia and endothelial cells), and RNA sequenced the cells right after purification. The signature matrix file, constructed from this cell-type specific RNA data, consists of “barcode genes that can discriminate each cell subset of interest in that tissue type, and can subsequently be used to impute cell fractions and cell expression profiles from bulk tissue transcriptomes”, according to the tutorial. Next, the mixture file was constructed, which consist of *DESeq2*-normalized gene expression values for all genes across all samples, for PFC and ACC data separately (see Appendix 2 on how the mixture file was constructed). Lastly, the gene subset file contains a list of genes of interest, here the Winter model genes.

The CIBERSORTx analysis was performed using the analysis module ‘3. Impute Cell Expression’ and analysis type ‘High-Resolution’. Optional merged class or ground truth files were not used. Batch correction (B-mode) was enabled and quantile normalization

was disabled. The window size used for deconvolution was 20. These decisions were made based on the guidelines presented in the tutorial.

Unfortunately, imputation of cell-type specific expressions did not provide coherent results for all the genes. This problem was present especially with astrocyte-specific expressions. Therefore, a decision was made to separately use both CIBERSORTx imputed expressions and bulk RNA expressions to perform the brain energy metabolism simulations. By using the cell-type specific expressions from CIBERSORTx, the differences between neuronal and astrocytic metabolism could be studied, and by using bulk RNA data, a higher number of genes was able to be included in the simulations.

Finally, the mean expressions of DE genes were calculated for SCZ and HC samples. The mean expressions in SCZ were compared to the mean expressions in HC in order to obtain coefficients which demonstrate how the mean expression of a gene has changed in schizophrenia. These coefficients were calculated for neurons and astrocytes separately when possible, using CIBERSORTx data, and when it was not available, DESeq2 normalized bulk data was used. This means that in the case of bulk data, it must be assumed that the difference in expression is caused by neurons or astrocytes alone, although this very likely does not reflect *in vivo* circumstances. Details on how these analyses were performed can be found in Appendix 2.

4.4 Brain energy metabolism simulations

COPASI is a software application which can be used for simulating and analyzing biochemical networks and systems, and it uses the Runge-Kutta integration method for simulating the ordinary differential equations [104]. In this work, COPASI simulator was used for modelling the brain energy metabolism by using the model presented in Winter et al. (2018) [101]. The COPASI file of the Winter model was downloaded from BioModels database (<https://www.ebi.ac.uk/biomodels/>; 10.9.2024), where the model is stored with an identifier MODEL1603240000.

The aim of the simulations was to study how the concentrations of key metabolites change in response to neuronal activation in schizophrenia vs the healthy brain. The metabolites which were studied are glucose (GLC), lactate (LAC), pyruvate (PYR), ATP, NAD and NADH. The concentration of each metabolite was studied in neurons and astrocytes separately. The simulation task used in COPASI is called a “Time Course analysis” which can be found in the CopasiUI, under the Tasks-tab. The desired

metabolites were added to a single plot under the Output Specifications → Plots in the CopasiUI.

The default Winter model (without modifying the model parameters) was used as a model of metabolism in the healthy brain. The schizophrenia simulations were done by adjusting the parameter(s) of each reaction of interest separately. The reaction parameters were adjusted either based on CIBERSORTx data and bulk data (separately), or solely based on bulk data if CIBERSORTx expressions were not available. Lastly, combination simulations were performed, where all CIBERSORTx or all bulk reactions were combined to investigate the cooperative action of the gene expression changes in schizophrenia.

During the preliminary simulations, it was noticed that the metabolite concentrations had not reached steady state at the time of stimulation in the schizophrenia simulations. Therefore, the model parameters had to be modified to make sure that the system is in steady state at the time of stimulation. In the original Winter model, the duration of the Time Course is 400 s, the interval size is 0.016 s, the stimulus occurs at $t_0 = 200$ s and the output is suppressed before 100 s. In order to allow the system to reach steady state before the stimulus, these parameters were changed so that the duration of the Time Course is 30,500 s, the interval size is 0.1 s, the stimulus occurs at $t_0 = 30,000$ s and the output is suppressed before 29,900 s. Modification of these parameters did not affect the results in the HC simulation. Furthermore, an interval size of 0.01 s was also tested, but since no noticeable differences were observed between the 0.1 s and 0.01 s intervals, the larger interval was chosen to reduce computational load.

The control case, every individual reaction and the combination were simulated by using the Time Course parameters, and the results were saved to a text file which contained time points as the rows and concentrations of the metabolites as the columns. The simulation results were plotted by using RStudio. Each plot showcases the concentration change of one metabolite as a function of time in schizophrenia vs healthy control. In addition, the concentrations were normalized (each concentration was divided by its baseline value), and the normalized concentrations were also plotted. The x-axis, which represents time, was adjusted to make the plots easier to read: instead of using 30,000 s as the stimulus time point, the x-axis was adjusted so that the stimulus happens at 0 s. The R code used for constructing the plots is presented in Appendix 2.

4.5 On the use of RNA sequencing data

The RNA sequencing data used for the differential expression (DE) analysis in this thesis is from the CommonMind Consortium [102]. The CommonMind data is not openly accessible. Here, the data was obtained under the distribution agreement between Tuomo Mäki-Marttunen and NIMH Center for Collaborative Genetic Studies.

The data were generated as part of the CommonMind Consortium supported by funding from Takeda Pharmaceuticals Company Limited, F. Hoffman-La Roche Ltd and NIH grants R01MH085542, R01MH093725, P50MH066392, P50MH080405, R01MH097276, RO1-MH-075916, P50M096891, P50MH084053S1, R37MH057881, AG02219, AG05138, MH06692, R01MH110921, R01MH109677, R01MH109897, U01MH103392, and contract HHSN271201300031C through IRP NIMH. Brain tissue for the study was obtained from the following brain bank collections: the Mount Sinai NIH Brain and Tissue Repository, the University of Pennsylvania Alzheimer's Disease Core Center, the University of Pittsburgh NeuroBioBank and Brain and Tissue Repositories, and the NIMH Human Brain Collection Core. CMC Leadership: Panos Roussos, Joseph Buxbaum, Andrew Chess, Schahram Akbarian, Vahram Haroutunian (Icahn School of Medicine at Mount Sinai), Bernie Devlin, David Lewis (University of Pittsburgh), Raquel Gur, Chang-Gyu Hahn (University of Pennsylvania), Enrico Domenici (University of Trento), Mette A. Peters, Solveig Sieberts (Sage Bionetworks), Thomas Lehner, Stefano Marenco, Barbara K. Lipska (NIMH).

5. RESULTS

5.1 Differentially expressed genes, protein expressions and selection of simulation genes

Statistics from the DE analyses of the hole PFC and ACC data sets are presented in Table 3. In addition, Winter model genes which are differentially expressed are presented in Table 4 (ACC) and Table 5 (PFC). The significance value for determining which genes are differentially expressed is $\alpha = 0.01$. In the PFC data set, out of the 85 Winter model genes, 23 are differentially expressed: seven genes are upregulated, and 16 genes are downregulated. In the ACC data set, only nine Winter model genes are differentially expressed: three genes are upregulated, and six genes are downregulated in SCZ compared to HC.

Table 3. *Statistics from the differential expression analyses of PFC and ACC.*

Gene count	Before filtering	After pre-filtering	After DESeq2 filtering	Upregulated	Downregulated
PFC	56,632	47,148	28,866	4343	2374
ACC	58,929	52,938	34,464	3247	1457

Table 4. *Differentially expressed Winter model genes in the ACC.*

Gene symbol	Log2 fold change	Adjusted p-value
ALDOB	0.34	1.67×10^{-5}
TALDO1	-0.18	5.21×10^{-4}
AK4	0.14	1.85×10^{-3}
LDHB	-0.25	2.14×10^{-3}
PGLS	-0.12	3.92×10^{-3}
TPI1	-0.22	4.93×10^{-3}
RPEL1	0.28	6.50×10^{-3}
ALDOC	-0.13	7.98×10^{-3}
AK6	-0.17	9.91×10^{-3}

Table 5. *Differentially expressed Winter model genes in the PFC.*

Gene symbol	Log2 fold change	Adjusted p-value
AK4	0.17	7.82×10^{-6}
AK1	-0.20	8.31×10^{-6}
PFKL	-0.20	1.31×10^{-5}
ALDOC	-0.21	1.64×10^{-5}
TALDO1	-0.18	2.32×10^{-5}
GAPDH	-0.17	6.48×10^{-5}
CKMT2	-0.18	7.44×10^{-5}
RPE	0.12	1.77×10^{-4}
ALDOB	0.30	2.06×10^{-4}
PGAM1	-0.18	3.97×10^{-4}
TPI1	-0.26	4.49×10^{-4}
LDHD	-0.17	6.05×10^{-4}
CKB	-0.17	6.09×10^{-4}
PGLS	-0.14	6.65×10^{-4}
TKTL2	0.33	9.95×10^{-4}
PFKM	-0.16	1.09×10^{-3}
AK8	-0.19	1.14×10^{-3}
SLC16A2	0.11	3.51×10^{-3}
ENO1	-0.11	4.54×10^{-3}
PKM	-0.14	5.24×10^{-3}
HK3	0.39	6.52×10^{-3}
SLC2A6	-0.13	6.60×10^{-3}
CKM	0.57	8.78×10^{-3}

Next, the protein expressions of DE genes were evaluated to see if there is enough evidence on protein level for the gene/protein to be included in the following simulations. The protein expressions of the DE genes are presented in Table 6. Note that Table 6

only includes genes/proteins which can be modeled in the Winter model. The Winter model includes reactions where multiple metabolic reactions are grouped into one (see Table 1), but only one of the proteins is included in the model as a parameter. As a result, ALDOB, ALDOC, ENO1, GAPDH, PGAM1 and TPI1 were eliminated from subsequent analyses. In addition, adenylate kinase genes (AK1, AK4, AK6 and AK8) were eliminated because they cannot be properly modeled: AKs catalyze both the forward and backward reactions, and some of the genes have increased and other decreased expression. Therefore, modulating the AK reaction based on the DE results would not yield coherent results.

Table 6. *Protein expressions of differentially expressed genes in neurons and astrocytes. Note that The Human Protein Atlas presents glial expression, not specifically astrocytic expression. Furthermore, the Human Protein Atlas expressions are from the cerebral cortex, not specifically from the PFC or the ACC.*

Gene symbol	Protein expression – The Human Protein Atlas		Protein expression – Other sources
	Neuron	Glia	
CKB	Not detected	Medium	CKB has low and selective expression in human neurons [105], but it is prominently expressed in human astrocytes [105] in the cerebral cortex [106].
CKM	Not detected	Not detected	CKM is not the isoform expressed in the brain [107].
CKMT2	Not detected	Not detected	CKMT2 is not the isoform expressed in the brain [107].
HK3	Not detected	Not detected	HK3 expression is relatively low in most tissues, and brain is not among the tissues with high expression [108].
LDHB	Medium	Low	Neurons express exclusively LDHB. In astrocytes, LDHB is expressed, but it is not the predominant isoform. [53]
LDHD	Low	Not detected	No additional information on LDHD protein expression was found.
PFKL	Low	Not detected	In the human cerebral cortex, only around 15 % of the PFK1 protein is of PFKL isoform [109]. There is little PFKL expression in human astrocytes [110].
PFKM	High	Low	In the human cerebral cortex, around 55 % of the PFK1 protein is of PFKM isoform [109]. There is little to no PFKM expression in astrocytes [110].

PGLS	Medium	Medium	No additional information on PGLS protein expression was found.
PKM	Medium	Low	Neurons express mainly PKM1, and astrocytes mainly PKM2, both encoded by PKM gene [111].
RPE	Medium	Low	No additional information on RPE protein expression was found.
RPEL1	Low	Not detected	No additional information on RPEL1 protein expression was found.
SLC2A6	Low	Not detected	There does not seem to be significant SLC2A6 protein expression in neurons or astrocytes [50].
SLC16A2	Not available	Not available	SLC16A2 is not expressed in the adult human neurons [112]. Information on astrocyte expression was not found.
TALDO1	Not available	Not available	In the brain, TALDO1 is selectively expressed in oligodendrocytes [113].
TKTL2	Not available	Not available	No additional information on TKTL2 protein expression was found.

CIBERSORTx tool was used to impute cell-type specific gene expression for neurons and astrocytes in order to improve the precision of the energy metabolism simulations. Unfortunately, CIBERSORTx could not impute cell-type specific expressions for all the genes, so bulk expression data had to be used alongside cell-type specific data. Table 7 presents the mean expression values (bulk and CIBERSORTx) of all the genes which could be simulated, and the corresponding coefficient values which were used to modify the Winter model parameters. Lastly, Figure 7 summarizes which genes were included in the brain energy simulations and which genes had to be eliminated and why.

Table 7. *Normalized expression values of all the genes which were used for the simulations. The coefficients were used to adjust the Winter model parameters.*

Gene symbol	Mean expression - SCZ	Mean expression - HC	Coefficient
Bulk data (PFC)			
PFKM	3532.88	4107.81	0.86
PKM	11776.87	13571.01	0.87
CKB	5544.50	6243.43	0.89
PGLS	134.28	149.54	0.90
RPE	778.74	742.40	1.05

CIBERSORTx data (PFC)			
PFKM (neuron)	6734.16	7041.54	0.96
PKM (neuron)	22125.64	23202.92	0.95
PGLS (neuron)	135.28	141.17	0.96
PGLS (astro)	160.77	159.69	0.99
Bulk data (ACC)			
LDHB	884.7	1143.7	0.77
PGLS	148.6	164.1	0.91
CIBERSORTx data (ACC)			
LDHB (neuron)	1755.64	2004.91	0.88
PGLS (neuron)	154.88	165.43	0.94
PGLS (astro)	154.52	156.97	0.98

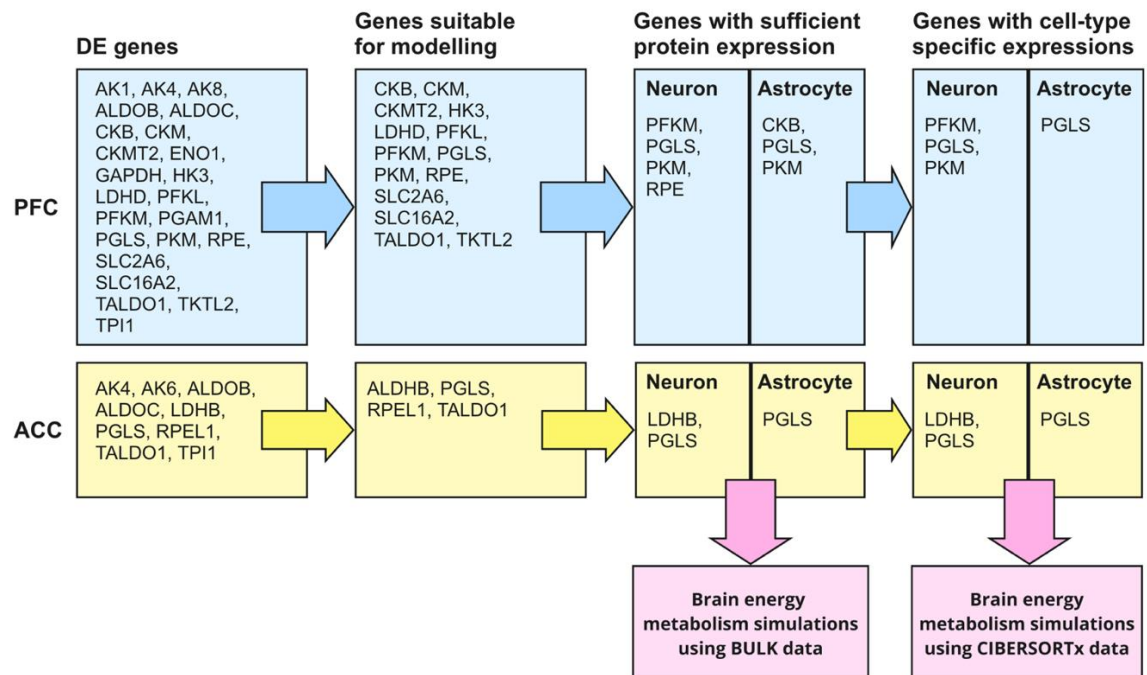


Figure 7. This figure illustrates why certain genes had to be eliminated, and which genes could be included in the brain energy metabolism simulations.

5.2 Simulation of altered expression of energy metabolism genes

The default Winter model was used to simulate the healthy brain, and these simulation results were used as the control. Next, the parameters of the Winter model were modified based on bulk and CIBERSORTx imputed gene expression data to model the schizophrenia cases. More information on which reactions and parameters were modified, is presented in Table 8.

Table 8. Winter model reactions, corresponding gene symbols, and the model parameters which were modified for the simulations. The parameters were modified based on coefficient values presented in Table 7.

Reaction	Gene symbol	Reaction name	Modified parameter
PFC			
$F6P + ATP \rightarrow 2\ GAP + ADP$	PFKM	PFK_neurons	k_PFK
$PEP + ADP \rightarrow PYR + ATP$	PKM	PK_neurons/ PK_astrocytes	k_PK
$PCr + ADP \leftrightarrow Cr + ATP$	CKB	CK_astrocytes	k1
$G6L \rightarrow P6G$	PGLS	SOL_neurons/ SOL_astrocytes	Vmax
$Ru5P \leftrightarrow X5P$	RPE	RPE_neurons	Vmax
ACC			
$PYR + NADH \leftrightarrow LAC + NAD$	LDHB	LDH_neurons	k2
$G6L \rightarrow P6G$	PGLS	SOL_neurons/ SOL_astrocytes	Vmax

Copasi simulator was used to study the concentration changes of metabolic species in neurons and astrocytes in response to neuronal activation. In the PFC simulations, four Winter model reactions could be modified based on CIBERSORTx imputed gene expressions, and seven reactions based on DE analysis results from bulk data. In the ACC simulations, the same three reactions could be modified using CIBERSORTx data and bulk data. Lastly, combination simulations were performed where the expression changes of all the genes were combined in the same simulation. These combination

ACC (CIBERSORTx)												
LDH_neurons	-	-	-	-	-	-	-		+	+	-	-
SOL_neurons												
SOL_astrocytes												
ACC (bulk)												
LDH_neurons	-	-	-	-	-	-	-		+	+	-	-
SOL_neurons												
SOL_astrocytes												

5.2.1 Prefrontal cortex (PFC) simulations

In the PFC simulations, the following Winter model reactions could be modified based on CIBERSORTx expressions: SOL_astrocytes (reaction rate altered based on change in PGLS expression), SOL_neurons (PGLS), PK_neurons (PKM) and PFK_neurons (PFKM). By using bulk data, simulations of RPE_neurons (RPE), CK_astrocytes (CKB) and PK_astrocytes (PKM) could also be added. Only decrease in neuronal PFKM caused significant changes in the metabolite concentrations, while the effects of other genes were found to be negligible. Figure 8 presents how decreased PFKM impacts absolute metabolite concentrations and Figure 9 displays the normalized concentrations. Downregulation of PFKM leads to increased baseline concentration of glucose and NAD, and decreased baseline concentration of ATP, lactate, pyruvate and NADH (Figure 8). In addition, decreased PFKM expression leads to alterations in the time courses of nearly all metabolite concentrations (Figure 9). Lastly, the combination PFC simulations (all gene expression changes simulated together) produced plots which are identical to PFKM simulation results, and therefore they are not presented separately.

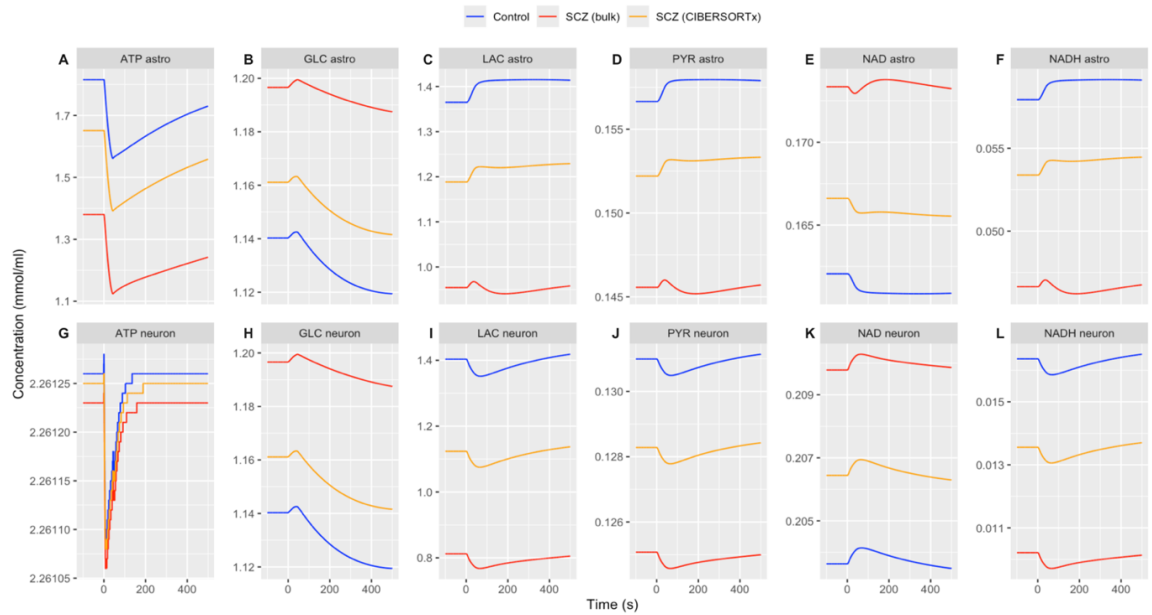


Figure 8. Effects of decreased neuronal PFKM expression on the **absolute** concentrations of central metabolites. The top row displays astrocytic concentrations of (a) ATP, (b) glucose, (c) lactate, (d) pyruvate, (e) NAD and (f) NADH. The bottom row displays neuronal concentrations of the same metabolites: (g) ATP, (h) glucose, (i) lactate, (j) pyruvate, (k) NAD and (l) NADH. “Bulk” refers to simulations where PFK_neurons reaction was altered based on bulk expression data and “CIBERSORTx” refers simulations where PFK_neurons was altered based on neuron-specific expression data (see additional details in Tables 7 and 8).

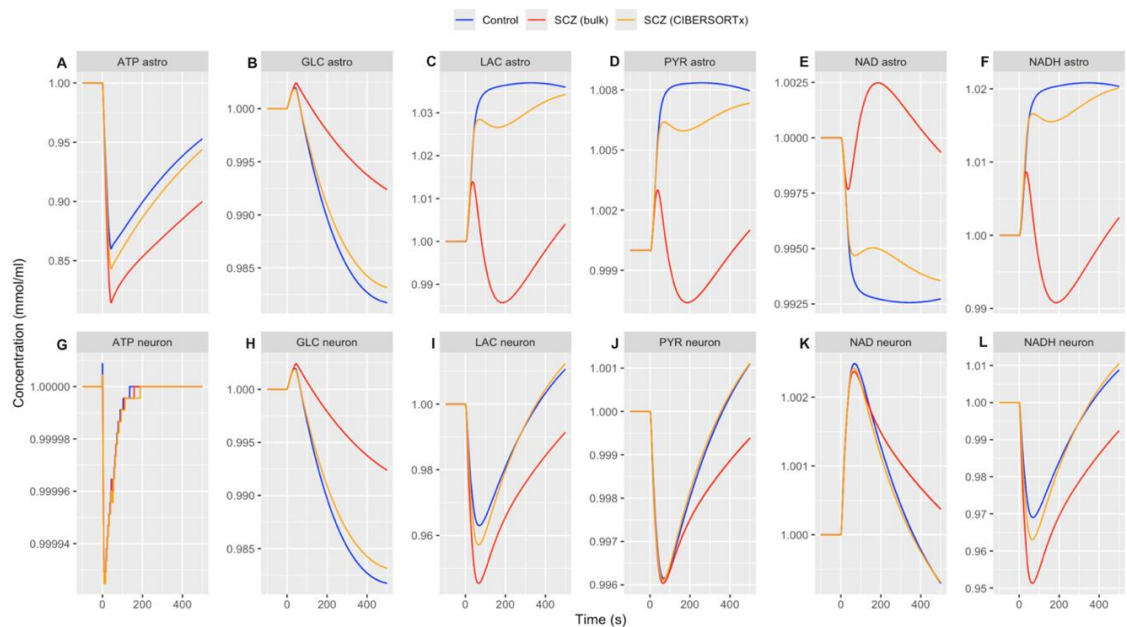


Figure 9. Effects of decreased neuronal PFKM expression on the **normalized** concentrations of central metabolites (each concentration divided by its baseline value). The top row displays astrocytic concentrations of (a) ATP, (b) glucose, (c) lactate, (d) pyruvate, (e) NAD and (f) NADH. The bottom row displays neuronal concentrations of the same metabolites: (g) ATP, (h) glucose, (i) lactate, (j) pyruvate, (k) NAD and (l) NADH.

5.2.2 Anterior cingulate cortex (ACC) simulations

The only three reactions which could be altered in the ACC simulations based on both CIBERSORTx and bulk gene expressions were SOL_neurons (PGLS gene), SOL_astrocytes (PGLS) and LDH_neurons (LDHB). Decreases in either neuronal or astrocytic PGLS expression did not affect any of the metabolite concentrations which were studied. However, decreased LDHB caused differences in neuronal pyruvate, NAD and NADH concentrations, and negligible differences in concentrations of the other metabolic species. Figure 10 presents the simulation results showing the effects of decreased LDHB on the absolute metabolite concentrations (a–c), and on the normalized concentrations (d–f). Downregulation of LDHB causes decreased baseline concentration of pyruvate and NADH, and increased baseline concentration of NAD (Figure 10 a–c). Additionally, there are small differences in the time courses of metabolite concentrations between SCZ (bulk and CIBERSORTx) and control (Figure 10 d–f).

It should be noted that LDH enzyme catalyzes both the conversion of pyruvate to lactate and back, simultaneously converting NADH to NAD and back. The Winter model has separate parameters for the forward and backward reactions. Based on literature ([114] and references therein), LDH1 isoenzyme, which is formed by four subunits encoded by LDHB gene, favors conversion of lactate to pyruvate (backward reaction). Since there is evidence that neurons express exclusively LDHB (LDH1) [53, 54], a decision was made to modify only the parameter of the backward reaction based on altered LDHB expression.

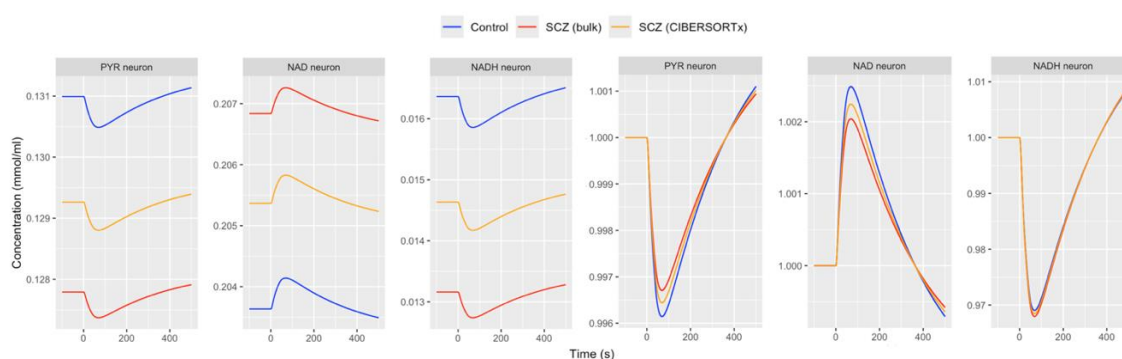


Figure 10. Effects of decreased neuronal LDHB expression on the **absolute** concentrations of (a) pyruvate, (b) NAD and (c) NADH, and **normalized** concentrations of (d) pyruvate, (e) NAD and (f) NADH.

6. DISCUSSION

6.1 Evaluation of materials and methods

6.1.1 Winter model

Brain energy metabolism model by Winter et al. was chosen to investigate how the concentrations of some key metabolites change in response to gene expression alterations in schizophrenia. Although this model was well suited for this purpose, it also had some limitations from the biological perspective. Firstly, the Winter model presents glycolysis, PPP and transport reactions of metabolites in detail, but mitochondrial ATP production is modelled only by a single reaction. Thus, central energy metabolism processes such as TCA cycle, oxidative phosphorylation and mitochondrial transport reactions were not able to be studied. This limitation is the largest downside of this model, since there is substantial evidence that in addition to cytosolic energy metabolism processes, mitochondrial processes are also disturbed in schizophrenia [23, 72, 74].

Secondly, the Winter model (and other brain energy metabolism models) does not represent any particular brain region, and instead it is a general model of brain energy metabolism. This means that no distinction between the PFC and the ACC was able to be made in the simulations (the initial model parameter values were identical in both control simulations). Nonetheless, there are regional differences in the energy metabolism in the brain [115–117], and optimally the model parameter values would reflect these regional differences. In the future, brain energy metabolism modelling could be improved by designing these region-specific models. However, obtaining brain region specific data is still challenging due to methodological limitations as well as disease heterogeneity between individuals.

In addition to limitations in brain region specificity, the cell types represented in the Winter model are limited. The Winter model includes only neurons and astrocytes, and thus the impact of other cell types in the brain, such as microglia and oligodendrocytes, cannot be taken into account. In addition, since synaptic neurotransmission is included in the model, it would be beneficial to distinguish pre- and postsynaptic sides of neurons. These opposing sides have distinct energy requirements and consequently the energy metabolism processes function differently on pre- and postsynaptic sides of neurons. By having separate compartments for pre- and postsynaptic sides of neurons, the distinct

metabolic profiles of these two sites could be modelled more accurately. Lastly, the transport reactions of central metabolites like glutamate, glucose and lactate could be portrayed more biologically accurately by including the of pre- and postsynaptic compartments.

Finally, the kinetic parameters of the Winter model vary between different metabolic reactions (see Table 8 for example). Therefore, different kinds of parameters were adjusted for the simulations. Since the parameters represent different reaction properties (for example k represents rate constant and V_{max} represents the maximum velocity of the reaction when the enzyme is fully saturated with the substrate), it is relevant to question should all these different parameters be adjusted in the same manner. Furthermore, adjusting these reaction rate parameters based on differences in gene expression may add unreliability to the simulation results, because these two elements are not directly proportional.

6.1.2 Limitations of post-mortem bulk RNA sequencing data

The DE analysis was performed using human bulk RNA-sequencing data from the CommonMind Consortium, which has its strengths and weaknesses. The strengths of this data include the large sample size in both data sets (PFC and ACC), and the fact that the data is from humans, which allows it to be used for the study of human diseases such as schizophrenia. On the other hand, the fact that it is post-mortem bulk data sets some limitations regarding the use of the data. First, the downsides of using post-mortem data include for example effects of post-mortem interval, mRNA integrity and the fact that post-mortem samples typically reflect the “mature” stages of schizophrenia [9]. Additionally, lifetime use of antipsychotics may affect post-mortem data: since the CommonMind data did not include information on medication status of the patients, the effects of different antipsychotics on the gene expression could not be taken into account in the DE analysis. Secondly, bulk mRNA data does not provide information on cell-type specific gene expression. Since bulk brain tissue contains a variety of cell types including neurons, different glial cells and endothelial cells, it is impossible to say based on bulk data how each cell type contributes to the gene expression differences associated with schizophrenia.

The Winter model used for simulating cytosolic energy metabolism has separate metabolic reactions to neurons and astrocytes, and therefore CIBERSORTx tool was used to impute neuron- and astrocyte-specific gene expressions from the bulk data.

Unfortunately, CIBERSORTx was not able to impute cell-type specific expressions for all genes, so bulk expressions were decided to be used alongside CIBERSORTx expressions. The challenge of using bulk data to calculate the expression differences between HC and SCZ lies in the necessity to assume that changes in gene expression are only driven by either neurons or astrocytes. However, this assumption is likely inaccurate because genes are typically expressed in many different cell types, and the expression may also be altered in multiple of them in schizophrenia. Thus, usage of bulk data to modify cell-type specific Winter model reactions may have reduced the accuracy of the simulation results. In an ideal situation, single-cell or single-nucleus sequencing data would have been available to be used for the DE analysis and subsequent brain energy metabolism simulations.

In addition to limitations of bulk data, limited information on protein expressions of Winter model genes added a challenge to the workflow. There is little information on protein level expressions on specific cell types (neurons and astrocytes) and on specific brain regions (PFC and ACC). The Human Protein Atlas provided some help, but it also has limited specificity: the database has information on neuronal protein expression, but instead of astrocyte-specific expressions, it provides only broader expression of glial cells. Secondly, The Human Protein Atlas does not have separate categories for PFC and ACC, and thus only cerebral cortex protein expressions could be obtained. In addition, when The Human Protein Atlas information was compared to literature, there were some discrepancies. Since protein expression data is limited, it is possible that some proteins that were excluded should have been included in the simulations and vice versa. In the future, the increase in brain-region and cell-type specific protein expression data should improve the accuracy of modelling.

Lastly, it is possible that although there are differences in mRNA expression between healthy individuals and schizophrenia patients, those differences may not be present on the protein level. For example, the translation of mRNA to protein can be controlled or inhibited, the translated protein can be degraded, or the activity of the protein is regulated or even inhibited. Therefore, additional information on the presence and activity of metabolic enzymes would also make the brain energy simulations more accurate.

6.2 Differentially expressed Winter model genes

6.2.1 Overview of the differential expression analysis results

The results from the DE analysis of Winter model genes reveal multiple interesting aspects of cytosolic brain energy metabolism from the PFC and the ACC. Firstly, there are about 2.5 times more differentially expressed genes in the PFC than in the ACC data set. This result indicates that energy metabolism may be more disturbed in the PFC than in the ACC in schizophrenia. However, the ratio of down- and upregulated genes is similar in both data sets: there are approximately twice as many downregulated genes as upregulated genes. Therefore, the bioenergetic disruptions seem to be more often connected to downregulation instead of upregulation of cytosolic energy metabolism genes.

Secondly, although 21 out of 85 genes in the Winter model gene set encode transporter proteins, only two of them (SLC2A6 and SLC16A2) are differentially expressed, both in the PFC. Furthermore, SLC2A6 encodes GLUT6 and SLC16A2 encodes MCT8 (also known as MCT7), and no significant evidence of these two proteins being expressed in neurons or astrocytes was found [50, 112]. Therefore, it seems like dysregulation of energy metabolism is more likely caused by problems in cytosolic energy metabolism enzymes than problems in metabolite transportation, and this hypothesis is in line with many proteomic studies which have not found significant differences in transporter protein expressions [70].

Information on which energy metabolism process each differentially expressed gene is involved in is presented in Table 10. Firstly, this figure illustrates that there are six genes which are differentially expressed in both data sets: ALDOB, ALDOC, TPI1, PGLS, TALDO1 and AK4. These genes are either upregulated (ALDOB, AK4) in both brain regions or downregulated (ALDOC, TPI1, PGLS, TALDO1) in both brain regions. Additionally, Table 10 shows that the majority of DE genes from the ACC are also differentially expressed in the PFC. However, note that no evidence of significant protein expression in neurons or astrocytes was found on ALDOB or TALDO1.

Table 10 also illustrates that PPP is the only group with a similar number of down- and upregulated genes in both brain regions. However, no evidence of significant protein expression of TKTL2, TALDO1 and RPEL1 was found. In addition, it was difficult to find brain region- and cell type-specific evidence of protein expression on PGLS and RPE.

Furthermore, even if altered expression of RPE and PGLS translates to protein level, it doesn't directly cause problems in energy production. Although PPP is a pathway parallel to glycolysis, it is not an energy production pathway, but instead its primary function is to produce precursors for nucleotide and amino acid biosynthesis. However, PPP also has an important role in preventing oxidative stress by generating NADPH which can reduce glutathione. Therefore, although disruption of PPP may not directly disturb ATP production, it may lead to increased oxidative stress for example by decreasing GSH concentration and causing mitochondrial dysfunction in schizophrenia [88].

Table 10. Differentially expressed genes in the PFC and the ACC, and which energy metabolism processes these genes are involved in. Underlined genes are upregulated, and the rest are downregulated in SCZ vs HC. Phosphotransferases refer to proteins which control ATP levels, such as adenylate kinase and creatine kinase.

glycolysis ENO1, GAPDH, <u>HK3</u> , LDHD, PFKL, PFKM, PKM, PGAM1	<u>ALDOB</u> , ALDOC, TPI1	glycolysis LDHB
phosphotransferases AK1, AK8, CKB, <u>CKM</u> , CKMT2	<u>AK4</u>	phosphotransferases AK6
pentose-phosphate pathway <u>RPE</u> , <u>TKTL2</u>	PGLS, TALDO1	pentose-phosphate pathway <u>RPEL1</u>
metabolite transporters SLC2A6, <u>SLC16A2</u>		metabolite transporters
PFC	both	ACC

6.2.2 Glycolytic enzymes and phosphotransferases

In the PFC data set, there are nine downregulated genes and only two upregulated genes related to glycolysis. Additionally, according to The Human Protein Atlas, the two upregulated genes (HK3 and ALDOB) are not expressed on the protein level in neurons or glia in the cerebral cortex. On the other hand, LDHD and PFKL are the only downregulated genes that are not significantly expressed on the protein level in neurons or astrocytes (other isoforms of these proteins are present in the brain). Thus, there are seven downregulated glycolysis genes with evidence of protein expression in the PFC in schizophrenia: ENO1, GAPDH, PFKM, PKM, PGAM1, ALDOC and TPI1. All these genes

have also been found to be differentially expressed in proteomic studies in the PFC (or more specifically in the DLPFC in some cases) in schizophrenia [75, 118–122].

Out of the glycolytic enzymes, ALDOC is the most frequently differentially expressed protein identified in proteomic studies [75, 119–122]. However, some of the studies report increased expression and others decreased expression of this protein in the PFC. These different findings may partly be explained by differences in the specific brain regions and their cell-types. In the brain, ALDOC is predominantly expressed by astrocytes [70], and therefore the astrocyte density of the post-mortem tissue can affect the results. One of the proteomic studies used brain tissue from dorsolateral white matter, which is rich in astrocytes, and this study found a decrease in ALDOC expression [120].

When it comes to the rest of the glycolytic enzymes, in some studies the protein expression was in line with the gene expression alterations identified in this thesis, and in other studies it was not: proteomic studies have identified decreased protein expression of ENO1 [75], PKM [75], PGAM1 [119] and TPI1 [120], but increased protein expression of GAPDH [118] and PFKM [118]. However, Sullivan and colleagues also found a decrease in PFK (isoform not specified) mRNA, and in addition a decrease in PFK activity in the DLPFC [76]. These results highlight the need for multimodal analyses that account for gene expression, protein expression, and protein activity in combination, as there may not always be a straightforward correlation between the three.

In the PFC, six phosphotransferase encoding genes were found to be differentially expressed between SCZ and HC: three of them are adenylate kinases (AKs) and the other three are creatine kinases (CKs). Alterations in AKs have not been strongly associated with schizophrenia: only one proteomic study has reported an increase of AK4 in the left DLPFC [121], and similarly an increase of AK4 was found on mRNA level in this thesis. However, studies have not found protein level alterations of AK1 (main isoform in the healthy brain [123, 124]) or AK8 (likely not expressed in the brain [123]) related to schizophrenia. Conversely, CKB (the main cytosolic isoform in the brain) has been associated with schizophrenia in a variety of studies. ³¹P-MRS studies have found a decrease in the rate-constant of the forward reaction of creatine kinase in the frontal regions [77–79], and proteomic studies have found altered expression of CKB in schizophrenia. Two studies from the frontal cortex have identified a decrease in CKB [125, 126] whereas two studies from the DLPFC have identified an increase in CKB [121,

127]. These results suggest that there are regional differences in the expression of CKB in the schizophrenic brain.

Finally, in the ACC data set there are four DE genes related to glycolysis. The only upregulated gene of these four (ALDOB) is not the isoform expressed in the brain. On the other hand, the remaining three genes (ALDOC, TPI1 and LDHB) are expressed on a protein level in the brain. Proteomic studies have found altered expression of ALDOC in the ACC: two studies have reported decreased expression [128, 129] and one study has reported increased expression [130] in schizophrenia. On the contrary, proteomic studies have not found altered expression of TPI1 or LDHB in the ACC, but instead in other brain areas [70]. Lastly, proteomic studies have not identified altered expression of AK4 or AK6 in the ACC, or in other brain regions (apart from the one study mentioned in the previous section). Overall, fewer studies have investigated the ACC compared to the PFC, which limits the knowledge on how gene and protein expression may be altered in this brain region in schizophrenia.

6.3 Effects of altered gene expression on central energy metabolites

6.3.1 Overview of the brain energy metabolism simulation results

In the PFC simulations, the gene expression changes were used to modify seven reactions using bulk data, and four reactions using CIBERSORTx data. In both cases, only the decrease of PFKM caused significant alterations in the metabolite concentrations between HC and SCZ. The simulation results from the ACC were similar: three reactions were modified based on both bulk and CIBERSORTx data, but only decreased LDHB caused any significant changes in the metabolite concentrations. When it came to the rest of the genes (PGLS, RPE, PKM and CKB), the concentration changes between HC and SCZ were insignificant based on both bulk and CIBERSORTx gene expressions in both brain regions.

PGLS and RPE are PPP enzymes, and as it was mentioned in Chapter 6.2.1, altered expression of these enzymes does not directly cause any concentration changes in any of the metabolites which were studied. Thus, the simulation results of PGLS and RPE were as expected. On the other hand, decreased expression of PKM and CKB in the PFC caused concentration changes in some of the metabolic species, but these changes were so small they were determined to be negligible (see Table 9). However, note that

decreased *neuronal* PKM caused changes only in some neuronal metabolite concentrations, whereas decreased *astrocytic* PKM caused changes in all astrocytic *and* neuronal metabolites, except for ATP. These PKM simulation results likely reflect the key role astrocytes have in supporting neuronal energy production. In conclusion, based on the simulation results of PKM and CKB it seems like decreased expression of either gene does not cause significant alterations in energy metabolism in schizophrenia. Furthermore, it is possible that decreased expression of these genes is a consequence of already present disturbed bioenergetics in the schizophrenic brain.

6.3.2 PFKM and LDHB

In the PFC, PFKM was one of the genes whose decreased expression could be simulated. There is evidence that PFKM is expressed in neurons but not in astrocytes, so only PFK_neurons reaction was altered in the Winter model. Simulation results portraying decreased expression of PFKM show significant alterations in all the metabolic species which were studied, except for neuronal ATP. Furthermore, metabolite concentrations were altered in both neurons and astrocytes which provides additional support for metabolic coupling of between these two cell types. Separate simulations were performed based on CIBERSORTx imputed gene expressions and bulk expressions. Since PFKM expression differences between SCZ and HC were larger in bulk data, the differences in metabolite concentrations were also expectedly larger in the bulk simulations. However, in some cases larger decrease in PFKM also created larger differences in the plot shapes.

Decreased PFKM caused alterations in the steady-state concentrations of all the studied metabolites: steady-state concentrations of lactate, pyruvate, ATP and NADH were smaller, and glucose and NAD were larger compared to the control. These results suggest that reduced PFKM expression slows down glycolysis, which leads to decreased pyruvate, lactate and ATP production, whereas glucose concentration is higher due to slower consumption. Additionally, conversion of NAD to NADH is slower, which explains their steady-state concentration differences. These results are expected for the neuronal concentrations, but the PFKM simulation results indicate that decreased *neuronal* PFKM actually causes larger alterations in the astrocytic metabolite concentrations (especially in response to neuronal activation) than the neuronal ones.

There is not a clear indication on why the decrease of neuronal PFKM causes such large alterations in astrocytic metabolite concentrations, but it may be at least partially

explained by how the PFK_neurons rate law is defined in the Winter model. PFK is a key enzyme of glycolysis, and it is controlled by multiple metabolites such as F2,6BP, ATP, ADP, and also pH [48]. Although many different formulations for the rate law of PFK have been suggested, the regulatory complexity of this enzyme makes the reaction very difficult to define in the modelling context [131]. Therefore, the simulation results of PFKM may be at least partly affected by the rate law which is used in the Winter model.

On the other hand, the simulation results of decreased neuronal LDHB in the ACC were more straightforward. The concentrations of only a few neuronal metabolites were altered compared to the control: steady-state pyruvate and NADH concentrations were decreased and NAD concentration increased in the LDHB simulations compared to the control. However, although LDHB typically converts lactate to pyruvate in neurons, decreased LDHB did not cause a significant alteration to lactate concentration. Lastly, it is important to remember that LDH enzyme catalyzes both the conversion of pyruvate to lactate and vice versa, and the direction of the reaction depends on the substrate concentrations. Since LDH-1 (encoded by LDHB) preferentially converts lactate into pyruvate in neurons, only the backward reaction was modified for the simulation. Nonetheless, the effects of the forward reaction on pyruvate and lactate concentrations, albeit smaller, cannot be completely forgotten or disregarded. However, since no studies investigating the concentrations of pyruvate, NAD and NADH in the ACC were found, these results provide new information on how decreased expression of LDHB may affect the concentrations of key metabolites in schizophrenia.

6.4 Summary

The aim of the DE analysis and the simulations of altered gene expression was to study which genes are differentially expressed in the PFC and the ACC in schizophrenia, and how these expression alterations affect the concentrations of central energy metabolites. The results showed that although a significant number of cytosolic energy metabolism genes were differentially expressed in schizophrenia, most of the genes that could be simulated did not cause significant changes in the metabolite concentrations. In addition, the DE analysis results showed that there are more DE genes in the PFC than the ACC, and that the majority of the DE genes are downregulated. These results are in line with the hypofrontality hypothesis of schizophrenia which suggests that there is lower energy metabolism in the anterior (especially the PFC) compared to the posterior brain regions [132]. However, if the simulation results are also taken into account, it can be hypothesized that the disruption of energy metabolism is not likely caused *only* by

alterations in genes which encode cytosolic energy metabolism proteins, but instead a variety of factors including redox imbalance, mitochondrial dysfunction and protein expression and activity contribute to disturbed bioenergetics in schizophrenia.

Lastly, the findings regarding cytosolic energy metabolism in schizophrenia are very heterogeneous and sometimes even contradictory. The variability in results can be partly attributed to limitations in study methods but furthermore, schizophrenia itself is an inherently heterogeneous disorder. There are multiple factors which create variability in the results such as differences in brain regions, disease state and antipsychotic status. Furthermore, it has been suggested that different antipsychotics may have varying effects on the bioenergetics in schizophrenia [10, 83]. Therefore, studying the differences between first episode vs chronic, and unmedicated vs medicated patients is especially important to understand how the dysregulation of cytosolic energy metabolism processes evolve over the course of the disorder, and how antipsychotics influence these processes. Due to these challenges, more research is still needed to better understand the connection between brain energy metabolism and schizophrenia. One way to do this is by improving the details of brain energy metabolism models.

The Winter model has a couple of instances where multiple metabolic reactions have been combined into one model reaction, and the rate of the reaction is controlled by only one parameter (see Table 1). In addition, the kinetic properties of different isoforms of the same enzyme are typically not taken into consideration in brain energy metabolism models. By formulating model reactions which are specific for each metabolic reaction and enzyme isoform, the accuracy of modelling based on gene expression changes can be significantly improved.

7. CONCLUSION

The purpose of this master's thesis was to study brain energy metabolism in schizophrenia. First, a computational model by Winter et al. was chosen to be used for the brain energy metabolism simulations. Before the simulations, post-mortem bulk mRNA sequencing data was used in a DE analysis to study the how the expression of cytosolic energy metabolism genes is altered in the PFC and the ACC in schizophrenia. The DE analysis revealed that the majority of the DE genes were downregulated in schizophrenia, and that there were significantly more DE genes in the PFC than the ACC. These results strengthen the evidence of regional differences in energy metabolism disruptions in the schizophrenic brain. Furthermore, the DE analysis results provide additional evidence that the PFC is a particularly significant brain region for studying energy metabolism disruptions in schizophrenia.

After the DE analysis, CIBERSORTx was used to impute cell-type specific gene expressions for neurons and astrocytes for the brain energy metabolism simulations. Since cell-type specific expression could not be imputed for all genes, bulk data was also used for the simulations. The aim of the simulations was to study how changes in gene expression influence the concentrations of central energy metabolites. The brain energy metabolism simulation results indicated that, in most cases, altered expression of a single gene does not significantly impact the concentrations of any studied metabolites. However, decreased expression of neuronally expressed PFKM in the PFC caused significant alterations in nearly all metabolites, both in neurons and astrocytes. Lastly, decreased expression of neuronal LDHB in the ACC also caused some significant alterations in the metabolite concentrations, but effects were limited to few neuronal metabolites.

To conclude, the results produced in this thesis support brain-region-specific energy metabolism disruptions in schizophrenia. The discrepancies between the results of this thesis and the existing literature on metabolite alterations suggest that changes in gene expression alone, at least those measured post-mortem, do not account for the brain energy disruptions associated with schizophrenia. Nonetheless, this thesis offers new insights into how alterations in cytosolic energy metabolism genes influence the concentrations of central metabolites in the PFC and the ACC of the schizophrenic brain.

REFERENCES

- [1] K. T. Mueser and S. R. McGurk, 'Schizophrenia', *Lancet*, vol. 363, no. 9426, pp. 2063–2072, Jun. 2004.
- [2] R. A. McCutcheon, T. Reis Marques, and O. D. Howes, 'Schizophrenia-An Overview', *JAMA Psychiatry*, vol. 77, no. 2, pp. 201–210, Feb. 2020.
- [3] O. D. Howes, B. R. Bukala, and K. Beck, 'Schizophrenia: from neurochemistry to circuits, symptoms and treatments', *Nat Rev Neurol*, vol. 20, no. 1, pp. 22–35, Jan. 2024.
- [4] O. D. Howes and E. Shatalina, 'Integrating the Neurodevelopmental and Dopamine Hypotheses of Schizophrenia and the Role of Cortical Excitation-Inhibition Balance', *Biol Psychiatry*, vol. 92, no. 6, pp. 501–513, Sep. 2022.
- [5] O. D. Howes and S. Kapur, 'The dopamine hypothesis of schizophrenia: version III--the final common pathway', *Schizophr Bull*, vol. 35, no. 3, pp. 549–562, May 2009.
- [6] O. D. Howes and R. M. Murray, 'Schizophrenia: an integrated sociodevelopmental-cognitive model', *Lancet*, vol. 383, no. 9929, pp. 1677–1687, May 2014.
- [7] O. B. Smeland, O. Frei, A. M. Dale, and O. A. Andreassen, 'The polygenic architecture of schizophrenia - rethinking pathogenesis and nosology', *Nat Rev Neurol*, vol. 16, no. 7, pp. 366–379, Jul. 2020.
- [8] A. Stein, C. Zhu, F. Du, and D. Öngür, 'Magnetic Resonance Spectroscopy Studies of Brain Energy Metabolism in Schizophrenia: Progression from Prodrome to Chronic Psychosis', *Curr Psychiatry Rep*, vol. 25, no. 11, pp. 659–669, Nov. 2023.
- [9] C. R. Sullivan, S. M. O'Donovan, R. E. McCullumsmith, and A. Ramsey, 'Defects in Bioenergetic Coupling in Schizophrenia', *Biol Psychiatry*, vol. 83, no. 9, pp. 739–750, May 2018.
- [10] N. D. Henkel, X. Wu, S. M. O'Donovan, E. A. Devine, J. M. Jiron, L. M. Rowland, Z. Sarnyai, A. J. Ramsey, Z. Wen, M. K. Hahn, and R. E. McCullumsmith, 'Schizophrenia: a disorder of broken brain bioenergetics', *Mol Psychiatry*, vol. 27, no. 5, pp. 2393–2404, May 2022.
- [11] J. P. Bolaños, 'Bioenergetics and redox adaptations of astrocytes to neuronal activity', *J Neurochem*, vol. 139 Suppl 2, no. Suppl Suppl 2, pp. 115–125, Oct. 2016.
- [12] G. Bonvento and J. P. Bolaños, 'Astrocyte-neuron metabolic cooperation shapes brain activity', *Cell Metab*, vol. 33, no. 8, pp. 1546–1564, Aug. 2021.
- [13] P. J. Magistretti and I. Allaman, 'A cellular perspective on brain energy metabolism and functional imaging', *Neuron*, vol. 86, no. 4, pp. 883–901, May 2015.
- [14] R. A. McCutcheon, R. S. E. Keefe, and P. K. McGuire, 'Cognitive impairment in schizophrenia: aetiology, pathophysiology, and treatment', *Mol Psychiatry*, vol. 28, no. 5, pp. 1902–1918, May 2023.

- [15] O. D. Howes, R. McCutcheon, M. J. Owen, and R. M. Murray, 'The Role of Genes, Stress, and Dopamine in the Development of Schizophrenia', *Biol Psychiatry*, vol. 81, no. 1, pp. 9–20, Jan. 2017.
- [16] J. L. Rapoport, J. N. Giedd, and N. Gogtay, 'Neurodevelopmental model of schizophrenia: update 2012', *Mol Psychiatry*, vol. 17, no. 12, pp. 1228–1238, Dec. 2012.
- [17] P. Chauhan, G. Kaur, R. Prasad, and H. Singh, 'Pharmacotherapy of schizophrenia: immunological aspects and potential role of immunotherapy', *Expert Rev Neurother*, vol. 21, no. 12, pp. 1441–1453, Dec. 2021.
- [18] B. S. Pruet and J. H. Meador-Woodruff, 'Evidence for altered energy metabolism, increased lactate, and decreased pH in schizophrenia brain: A focused review and meta-analysis of human postmortem and magnetic resonance spectroscopy studies', *Schizophr Res*, vol. 223, pp. 29–42, Sep. 2020.
- [19] B. K. Y. Bitanirwe and T.-U. W. Woo, 'Oxidative stress in schizophrenia: an integrated approach', *Neurosci Biobehav Rev*, vol. 35, no. 3, pp. 878–893, Jan. 2011.
- [20] C. Missale, S. R. Nash, S. W. Robinson, M. Jaber, and M. G. Caron, 'Dopamine receptors: from structure to function', *Physiol Rev*, vol. 78, no. 1, pp. 189–225, Jan. 1998.
- [21] H. Xu and F. Yang, 'The interplay of dopamine metabolism abnormalities and mitochondrial defects in the pathogenesis of schizophrenia', *Transl Psychiatry*, vol. 12, no. 1, p. 464, Nov. 2022.
- [22] A. A. Grace, 'Dysregulation of the dopamine system in the pathophysiology of schizophrenia and depression', *Nat Rev Neurosci*, vol. 17, no. 8, pp. 524–532, Aug. 2016.
- [23] A. Rajasekaran, G. Venkatasubramanian, M. Berk, and M. Debnath, 'Mitochondrial dysfunction in schizophrenia: pathways, mechanisms and implications', *Neurosci Biobehav Rev*, vol. 48, pp. 10–21, Jan. 2015.
- [24] B. Moghaddam and D. Javitt, 'From revolution to evolution: the glutamate hypothesis of schizophrenia and its implication for treatment', *Neuropsychopharmacology*, vol. 37, no. 1, pp. 4–15, Jan. 2012.
- [25] R. M. Ryan, S. L. Ingram, and A. Scimemi, 'Regulation of Glutamate, GABA and Dopamine Transporter Uptake, Surface Mobility and Expression', *Front Cell Neurosci*, vol. 15, no. 13, p. 670346, Apr. 2021.
- [26] N. G. Bowery and T. G. Smart, 'GABA and glycine as neurotransmitters: a brief history', *Br J Pharmacol*, vol. 147 Suppl 1, no. Suppl 1, pp. S109–119, Jan. 2006.
- [27] Y. Uno and J. T. Coyle, 'Glutamate hypothesis in schizophrenia', *Psychiatry Clin Neurosci*, vol. 73, no. 5, pp. 204–215, May 2019.
- [28] A. Egerton, A. A. Grace, J. Stone, M. G. Bossong, M. Sand, and P. McGuire, 'Glutamate in schizophrenia: Neurodevelopmental perspectives and drug development', *Schizophr Res*, vol. 223, pp. 59–70, Sep. 2020.
- [29] R. A. McCutcheon, J. H. Krystal, and O. D. Howes, 'Dopamine and glutamate in schizophrenia: biology, symptoms and treatment', *World Psychiatry*, vol. 19, no. 1, pp. 15–33, Feb. 2020.

- [30] O. Howes, R. McCutcheon, and J. Stone, 'Glutamate and dopamine in schizophrenia: an update for the 21st century', *J Psychopharmacol*, vol. 29, no. 2, pp. 97–115, Feb. 2015.
- [31] K. Merritt *et al.*, 'Variability and magnitude of brain glutamate levels in schizophrenia: a meta and mega-analysis', *Mol Psychiatry*, vol. 28, no. 5, pp. 2039–2048, May 2023.
- [32] S. F. Taylor and I. F. Tso, 'GABA abnormalities in schizophrenia: a methodological review of in vivo studies', *Schizophr Res*, vol. 167, no. 1–3, pp. 84–90, Sep. 2015.
- [33] J. C. de Jonge, C. H. Vinkers, H. E. Hulshoff Pol, and A. Marsman, 'GABAergic Mechanisms in Schizophrenia: Linking Postmortem and In Vivo Studies', *Front Psychiatry*, vol. 8, no. 11, p. 118, Aug. 2017.
- [34] S. A. Buck, M. Quincy Erickson-Oberg, R. W. Logan, and Z. Freyberg, 'Relevance of interactions between dopamine and glutamate neurotransmission in schizophrenia', *Mol Psychiatry*, vol. 27, no. 9, pp. 3583–3591, Sep. 2022.
- [35] M. Kokkinou, E. E. Irvine, D. R. Bonsall, S. Natesan, L. A. Wells, M. Smith, J. Glegola, E. J. Paul, K. Tossell, M. Veronese, S. Khadayate, N. Dedic, S. C. Hopkins, M. A. Ungless, D. J. Withers, and O. D. Howes, 'Reproducing the dopamine pathophysiology of schizophrenia and approaches to ameliorate it: a translational imaging study with ketamine', *Mol Psychiatry*, vol. 26, no. 6, pp. 2562–2576, Jun. 2021.
- [36] C. Bortolon, A. Macgregor, D. Capdevielle, and S. Raffard, 'Apathy in schizophrenia: A review of neuropsychological and neuroanatomical studies', *Neuropsychologia*, vol. 118, no. Pt B, pp. 22–33, Sep. 2018.
- [37] F. S. Bersani, A. Minichino, M. Fojanesi, M. Gallo, G. Maglio, G. Valeriani, M. Biondi, and P. B. Fitzgerald, 'Cingulate Cortex in Schizophrenia: its relation with negative symptoms and psychotic onset. A review study', *Eur Rev Med Pharmacol Sci*, vol. 18, no. 22, pp. 3354–3367, Nov. 2014.
- [38] S. Jauhar, R. McCutcheon, F. Borgan, M. Veronese, M. Nour, F. Pepper, M. Rogdaki, J. Stone, A. Edgerton, F. Turkheimer, P. McGuire, and O. D. Howes, 'The relationship between cortical glutamate and striatal dopamine in first-episode psychosis: a cross-sectional multimodal PET and magnetic resonance spectroscopy imaging study', *Lancet Psychiatry*, vol. 5, no. 10, pp. 816–823, Oct. 2018.
- [39] A. G. Dietz, S. A. Goldman, and M. Nedergaard, 'Glial cells in schizophrenia: a unified hypothesis', *Lancet Psychiatry*, vol. 7, no. 3, pp. 272–281, Mar. 2020.
- [40] H.-G. Bernstein, J. Steiner, P. C. Guest, H. Dobrowolny, and B. Bogerts, 'Glial cells as key players in schizophrenia pathology: recent insights and concepts of therapy', *Schizophrenia Research*, vol. 161, no. 1, pp. 4–18, Jan. 2015.
- [41] E. C. de Oliveira Figueiredo, C. Cali, F. Petrelli, and P. Bezzi, 'Emerging evidence for astrocyte dysfunction in schizophrenia', *Glia*, vol. 70, no. 9, pp. 1585–1604, Sep. 2022.
- [42] T. Notter, 'Astrocytes in schizophrenia', *Brain Neurosci Adv*, vol. 5, no. 27, p. 23982128211009148, Apr. 2021.
- [43] A. Lima, V. M. Sardinha, A. F. Oliveira, M. Reis, C. Mota, M. A. Silva, F. Marques, J. J. Cerqueira, L. Pinto, N. Sousa, and J. F. Oliveira, 'Astrocyte pathology in the prefrontal cortex impairs the cognitive function of rats', *Mol Psychiatry*, vol. 19, no. 7, pp. 834–841, Jul. 2014.

- [44] H. S. Lee, A. Ghetti, A. Pinto-Duarte, X. Wang, G. Dziewczapolski, G. Galimi, S. Huitron-Resendiz, J. C. Piña-Crespo, A. J. Roberts, I. M. Verma, T. J. Sejnowski, and S. F. Heinemann, 'Astrocytes contribute to gamma oscillations and recognition memory', *Proc Natl Acad Sci U S A*, vol. 111, no. 32, pp. E3343-3352, Aug. 2014.
- [45] M. Bélanger, I. Allaman, and P. J. Magistretti, 'Brain energy metabolism: focus on astrocyte-neuron metabolic cooperation', *Cell Metab*, vol. 14, no. 6, pp. 724–738, Dec. 2011.
- [46] L. F. Barros, A. Brown, and R. A. Swanson, 'Glia in brain energy metabolism: A perspective', *Glia*, vol. 66, no. 6, pp. 1134–1137, Jun. 2018.
- [47] J. J. Harris, R. Jolivet, and D. Attwell, 'Synaptic energy use and supply', *Neuron*, vol. 75, no. 5, pp. 762–777, Sep. 2012.
- [48] G. A. Dienel, 'Brain Glucose Metabolism: Integration of Energetics with Function', *Physiol Rev*, vol. 99, no. 1, pp. 949–1045, Jan. 2019.
- [49] P. J. Magistretti and I. Allaman, 'Lactate in the brain: from metabolic end-product to signalling molecule', *Nat Rev Neurosci*, vol. 19, no. 4, pp. 235–249, Apr. 2018.
- [50] H. Koepsell, 'Glucose transporters in brain in health and disease', *Pflugers Arch*, vol. 472, no. 9, pp. 1299–1343, Sep. 2020.
- [51] Y. Zhang, K. Chen, S. A. Sloan, M. L. Bennett, A. R. Scholze, S. O'Keeffe, H. P. Phatnani, P. Guarnieri, C. Caneda, N. Ruderisch, S. Deng, S. A. Liddelow, C. Zhang, R. Daneman, T. Maniatis, B. A. Barres, and J. Q. Wu, 'An RNA-sequencing transcriptome and splicing database of glia, neurons, and vascular cells of the cerebral cortex', *J Neurosci*, vol. 34, no. 36, pp. 11929–11947, Sep. 2014.
- [52] A. Herrero-Mendez, A. Almeida, E. Fernández, C. Maestre, S. Moncada, and J. P. Bolaños, 'The bioenergetic and antioxidant status of neurons is controlled by continuous degradation of a key glycolytic enzyme by APC/C-Cdh1', *Nat Cell Biol*, vol. 11, no. 6, pp. 747–752, Jun. 2009.
- [53] P. G. Bittar, Y. Charnay, L. Pellerin, C. Bouras, and P. J. Magistretti, 'Selective Distribution of Lactate Dehydrogenase Isoenzymes in Neurons and Astrocytes of Human Brain', *J Cereb Blood Flow Metab*, vol. 16, no. 6, pp. 1079–1089, Nov. 1996.
- [54] J. D. Laughton, P. Bittar, Y. Charnay, L. Pellerin, E. Kovari, P. J. Magistretti, and C. Bouras, 'Metabolic compartmentalization in the human cortex and hippocampus: evidence for a cell- and region-specific localization of lactate dehydrogenase 5 and pyruvate dehydrogenase', *BMC Neurosci*, vol. 8, no. 23, p. 35, May 2007.
- [55] P. S. Ward and C. B. Thompson, 'Metabolic reprogramming: a cancer hallmark even warburg did not anticipate', *Cancer Cell*, vol. 21, no. 3, pp. 297–308, Mar. 2012.
- [56] G. A. Brooks, 'The Science and Translation of Lactate Shuttle Theory', *Cell Metab*, vol. 27, no. 4, pp. 757–785, Apr. 2018.
- [57] A. Schurr, 'Cerebral glycolysis: a century of persistent misunderstanding and misconception', *Front Neurosci*, vol. 8, no. 19, p. 360, Nov. 2014.

- [58] B. S. Ferguson, M. J. Rogatzki, M. L. Goodwin, D. A. Kane, Z. Rightmire, and L. B. Gladden, 'Lactate metabolism: historical context, prior misinterpretations, and current understanding', *Eur J Appl Physiol*, vol. 118, no. 4, pp. 691–728, Apr. 2018.
- [59] S. N. Vaishnavi, A. G. Vlassenko, M. M. Rundle, A. Z. Snyder, M. A. Mintun, and M. E. Raichle, 'Regional aerobic glycolysis in the human brain', *Proc Natl Acad Sci U S A*, vol. 107, no. 41, pp. 17757–17762, Oct. 2010.
- [60] F. Boumezbeur, K. F. Petersen, G. W. Cline, G. F. Mason, K. L. Behar, G. I. Shulman, and D. L. Rothman, 'The contribution of blood lactate to brain energy metabolism in humans measured by dynamic ^{13}C nuclear magnetic resonance spectroscopy', *J Neurosci*, vol. 30, no. 42, pp. 13983–13991, Oct. 2010.
- [61] L. Pellerin and P. J. Magistretti, 'Glutamate uptake into astrocytes stimulates aerobic glycolysis: a mechanism coupling neuronal activity to glucose utilization', *Proc Natl Acad Sci U S A*, vol. 91, no. 22, pp. 10625–10629, Oct. 1994.
- [62] G. A. Dienel, 'Brain lactate metabolism: the discoveries and the controversies', *J Cereb Blood Flow Metab*, vol. 32, no. 7, pp. 1107–1138, Jul. 2012.
- [63] C.-P. Chih and E. L. Roberts, 'Energy Substrates for Neurons during Neural Activity: A Critical Review of the Astrocyte-Neuron Lactate Shuttle Hypothesis', *J Cereb Blood Flow Metab*, vol. 23, no. 11, pp. 1263–1281, Nov. 2003.
- [64] P. Mächler, M. T. Wyss, M. Elsayed, J. Stobart, R. Gutierrez, A. von Faber-Castell, V. Kaelin, M. Zuend, A. San Martín, I. Romero-Gómez, F. Baeza-Lehnert, S. Lengacher, B. L. Schneider, P. Aebischer, P. J. Magistretti, L. F. Barros, and B. Weber, 'In Vivo Evidence for a Lactate Gradient from Astrocytes to Neurons', *Cell Metab*, vol. 23, no. 1, pp. 94–102, Jan. 2016.
- [65] D. Jimenez-Blasco, P. Santofimia-Castaño, A. Gonzalez, A. Almeida, and J. P. Bolaños, 'Astrocyte NMDA receptors' activity sustains neuronal survival through a Cdk5-Nrf2 pathway', *Cell Death Differ*, vol. 22, no. 11, pp. 1877–1889, Nov. 2015.
- [66] D. Martins-de-Souza, L. W. Harris, P. C. Guest, and S. Bahn, 'The role of energy metabolism dysfunction and oxidative stress in schizophrenia revealed by proteomics', *Antioxid Redox Signal*, vol. 15, no. 7, pp. 2067–2079, Oct. 2011.
- [67] S.-Y. Kim, B. M. Cohen, X. Chen, S. E. Lukas, A. K. Shinn, A. C. Yuksel, T. Li, F. Du, and D. Öngür, 'Redox Dysregulation in Schizophrenia Revealed by in vivo NAD⁺/NADH Measurement', *Schizophr Bull*, vol. 43, no. 1, pp. 197–204, Jan. 2017.
- [68] G. Morris, K. R. Walder, M. Berk, W. Marx, A. J. Walker, M. Maes, and B. K. Puri, 'The interplay between oxidative stress and bioenergetic failure in neuropsychiatric illnesses: can we explain it and can we treat it?', *Mol Biol Rep*, vol. 47, no. 7, pp. 5587–5620, Jul. 2020.
- [69] T. Pillinger, R. A. McCutcheon, L. Vano, Y. Mizuno, A. Arumham, G. Hindley, K. Beck, S. Natesan, O. Efthimiou, A. Cipriani, and O. D. Howes, 'Comparative effects of 18 antipsychotics on metabolic function in patients with schizophrenia, predictors of metabolic dysregulation, and association with psychopathology: a systematic review and network meta-analysis', *The Lancet Psychiatry*, vol. 7, no. 1, pp. 64–77, Jan. 2020.
- [70] K. Davaliev, I. Maleva Kostovska, and A. J. Dwork, 'Proteomics Research in Schizophrenia', *Front Cell Neurosci*, vol. 10, no. 16, p. 18, Feb. 2016.

- [71] J. M. Nascimento and D. Martins-de-Souza, 'The proteome of schizophrenia', *NPJ Schizophr*, vol. 1, no. 4, p. 14003, Mar. 2015.
- [72] R. C. Roberts, 'Postmortem studies on mitochondria in schizophrenia', *Schizophr Res*, vol. 187, no. 187, pp. 17–25, Sep. 2017.
- [73] H. Manji, T. Kato, N. A. Di Prospero, S. Ness, M. F. Beal, M. Krams, and G. Chen, 'Impaired mitochondrial function in psychiatric disorders', *Nat Rev Neurosci*, vol. 13, no. 5, pp. 293–307, Apr. 2012.
- [74] I. Fizíková, J. Dragašek, and P. Račay, 'Mitochondrial Dysfunction, Altered Mitochondrial Oxygen, and Energy Metabolism Associated with the Pathogenesis of Schizophrenia', *Int J Mol Sci*, vol. 24, no. 9, p. 7991, Apr. 2023.
- [75] S. Prabakaran, J. E. Swatton, M. M. Ryan, S. J. Huffaker, J. T.-J. Huang, J. L. Griffin, M. Wayland, T. Freeman, F. Dudbridge, K. S. Lilley, N. A. Karp, S. Hester, D. Tkachev, M. L. Mimmack, R. H. Yolken, M. J. Webster, E. F. Torrey, and S. Bahn, 'Mitochondrial dysfunction in schizophrenia: evidence for compromised brain metabolism and oxidative stress', *Mol Psychiatry*, vol. 9, no. 7, pp. 684–697, 643, Jul. 2004.
- [76] C. R. Sullivan, R. H. Koene, K. Hasselfeld, S. M. O'Donovan, A. Ramsey, and R. E. McCullumsmith, 'Neuron-specific deficits of bioenergetic processes in the dorsolateral prefrontal cortex in schizophrenia', *Mol Psychiatry*, vol. 24, no. 9, pp. 1319–1328, Sep. 2019.
- [77] C. Yuksel, X. Chen, V.-A. Chouinard, L. D. Nickerson, M. Gardner, T. Cohen, D. Öngür, and F. Du, 'Abnormal Brain Bioenergetics in First-Episode Psychosis', *Schizophr Bull Open*, vol. 2, no. 1, p. sgaa073, Jan. 2021.
- [78] F. Du, A. J. Cooper, T. Thida, S. Sehovic, S. E. Lukas, B. M. Cohen, X. Zhang, and D. Öngür, 'In Vivo Evidence for Cerebral Bioenergetic Abnormalities in Schizophrenia Measured Using ^{31}P Magnetization Transfer Spectroscopy', *JAMA Psychiatry*, vol. 71, no. 1, pp. 19–27, Jan. 2014.
- [79] X. Song, X. Chen, C. Yuksel, J. Yuan, D. A. Pizzagalli, B. Forester, D. Öngür, and F. Du, 'Bioenergetics and abnormal functional connectivity in psychotic disorders', *Mol Psychiatry*, vol. 26, no. 6, pp. 2483–2492, Jun. 2021.
- [80] D. Ongür, A. P. Prescott, J. E. Jensen, B. M. Cohen, and P. F. Renshaw, 'Creatine abnormalities in schizophrenia and bipolar disorder', *Psychiatry Res*, vol. 172, no. 1, pp. 44–48, Apr. 2009.
- [81] C. L. Beasley, K. Pennington, A. Behan, R. Wait, M. J. Dunn, and D. Cotter, 'Proteomic analysis of the anterior cingulate cortex in the major psychiatric disorders: Evidence for disease-associated changes', *Proteomics*, vol. 6, no. 11, pp. 3414–3425, Jun. 2006.
- [82] S. A. Wijtenburg, M. Wang, S. A. Korenic, S. Chen, P. B. Barker, and L. M. Rowland, 'Metabolite Alterations in Adults With Schizophrenia, First Degree Relatives, and Healthy Controls: A Multi-Region 7T MRS Study', *Front. Psychiatry*, vol. 12, no. 19, p. 656459, May 2021.
- [83] Y. Zhang, L. Tong, L. Ma, H. Ye, S. Zeng, S. Zhang, Y. Ding, W. Wang, and T. Bao, 'Progress in The Research of Lactate Metabolism Disruption And Astrocyte-Neuron Lactate Shuttle Impairment in Schizophrenia: A Comprehensive Review', *Advanced Biology*, vol. 8, no. 6, p. e2300409, Jun. 2024.

- [84] S. Liu, L. Zhang, X. Fan, G. Wang, Q. Liu, Y. Yang, M. Shao, M. Song, W. Li, L. Lv, X. Su, 'Lactate levels in the brain and blood of schizophrenia patients: A systematic review and meta-analysis', *Schizophrenia Research*, vol. 264, no. 264, pp. 29–38, Feb. 2024.
- [85] L. M. Rowland, S. Pradhan, S. Korenic, S. A. Wijtenburg, L. E. Hong, R. A. Edden, and P. B. Barker, 'Elevated brain lactate in schizophrenia: a 7 T magnetic resonance spectroscopy study', *Transl Psychiatry*, vol. 6, no. 11, pp. e967–e967, Nov. 2016.
- [86] A. M. Wang, S. Pradhan, J. M. Coughlin, A. Trivedi, S. L. DuBois, J. L. Crawford, T. W. Sedlak, F. C. Nucifora, G. Nestadt, L. G. Nucifora, D. J. Schretlen, A. Sawa, and P. B. Barker, 'Assessing Brain Metabolism With 7-T Proton Magnetic Resonance Spectroscopy in Patients With First-Episode Psychosis', *JAMA Psychiatry*, vol. 76, no. 3, pp. 314–323, Mar. 2019.
- [87] H.-J. Park, I. Choi, and K.-H. Leem, 'Decreased Brain pH and Pathophysiology in Schizophrenia', *Int J Mol Sci*, vol. 22, no. 16, p. 8358, Aug. 2021.
- [88] Y. Kim, K. C. Vadodaria, Z. Lenkei, T. Kato, F. H. Gage, M. C. Marchetto, and R. Santos, 'Mitochondria, Metabolism, and Redox Mechanisms in Psychiatric Disorders', *Antioxid Redox Signal*, vol. 31, no. 4, pp. 275–317, Aug. 2019.
- [89] J. K. Yao and M. S. Keshavan, 'Antioxidants, redox signaling, and pathophysiology in schizophrenia: an integrative view', *Antioxid Redox Signal*, vol. 15, no. 7, pp. 2011–2035, Oct. 2011.
- [90] V.-A. Chouinard, S.-Y. Kim, L. Valeri, C. Yuksel, K. P. Ryan, G. Chouinard, B. M. Cohen, F. Du, D. Öngür, 'Brain bioenergetics and redox state measured by 31 P magnetic resonance spectroscopy in unaffected siblings of patients with psychotic disorders', *Schizophrenia Research*, vol. 187, no. 187, pp. 11–16, Sep. 2017.
- [91] M. Bošković, T. Vovk, B. Kores Plesničar, and I. Grabnar, 'Oxidative stress in schizophrenia', *Curr Neuropharmacol*, vol. 9, no. 2, pp. 301–312, Jun. 2011.
- [92] T. K. Das, A. Javadzadeh, A. Dey, P. Sabesan, J. Théberge, J. Radua, L. Palaniyappan, 'Antioxidant defense in schizophrenia and bipolar disorder: A meta-analysis of MRS studies of anterior cingulate glutathione', *Progress in Neuro-Psychopharmacology and Biological Psychiatry*, vol. 91, no. 20, pp. 94–102, Apr. 2019.
- [93] V. J. Sydnor and D. R. Roalf, 'A meta-analysis of ultra-high field glutamate, glutamine, GABA and glutathione 1HMRS in psychosis: Implications for studies of psychosis risk', *Schizophrenia Research*, vol. 226, pp. 61–69, Dec. 2020.
- [94] D. Matsuzawa, T. Obata, Y. Shirayama, H. Nonaka, Y. Kanazawa, E. Yoshitome, J. Takanashi, T. Matsuda, E. Shimizu, H. Ikehira, M. Iyo, and K. Hashimoto, 'Negative correlation between brain glutathione level and negative symptoms in schizophrenia: a 3T 1H-MRS study', *PLoS One*, vol. 3, no. 4, p. e1944, Apr. 2008.
- [95] A. Aubert, R. Costalat, and R. Valabrègue, 'Modelling of the coupling between brain electrical activity and metabolism', *Acta Biotheor*, vol. 49, no. 4, pp. 301–326, Dec. 2001.
- [96] E. Somersalo, Y. Cheng, and D. Calvetti, 'The Metabolism of Neurons and Astrocytes Through Mathematical Models', *Ann Biomed Eng*, vol. 40, no. 11, pp. 2328–2344, Nov. 2012.
- [97] D. Sterratt, Ed., *Principles of computational modelling in neuroscience*. Cambridge ; New York: Cambridge University Press, 2011.

- [98] E. Klipp and W. Liebermeister, 'Mathematical modeling of intracellular signaling pathways', *BMC Neurosci*, vol. 7, no. S1, p. S10, Oct. 2006.
- [99] R. Jolivet, I. Allaman, L. Pellerin, P. J. Magistretti, and B. Weber, 'Comment on recent modeling studies of astrocyte-neuron metabolic interactions', *J Cereb Blood Flow Metab*, vol. 30, no. 12, pp. 1982–1986, Dec. 2010.
- [100] S. Mangia, M. DiNuzzo, F. Giove, A. Carruthers, I. A. Simpson, and S. J. Vannucci, 'Response to "comment on recent modeling studies of astrocyte-neuron metabolic interactions": much ado about nothing', *J Cereb Blood Flow Metab*, vol. 31, no. 6, pp. 1346–1353, Jun. 2011.
- [101] F. Winter, C. Bludszweit-Philipp, and O. Wolkenhauer, 'Mathematical analysis of the influence of brain metabolism on the BOLD signal in Alzheimer's disease', *J Cereb Blood Flow Metab*, vol. 38, no. 2, pp. 304–316, Feb. 2018.
- [102] G. E. Hoffman, J. Bendl, G. Voloudakis, K. S. Montgomery, L. Sloofman, Y.-C. Wang, H. R. Shah, M. E. Hauberg, J. S. Johnson, K. Girdhar, L. Song, J. F. Fullard, R. Kramer, C.-G. Hahn, R. Gur, S. Marengo, B. K. Lipska, D. A. Lewis, V. Haroutunian, S. Hemby, P. Sullivan, S. Akbarian, A. Chess, J. D. Buxbaum, G. E. Crawford, E. Domenici, B. Devlin, S. K. Sieberts, M. A. Peters, and P. Roussos, 'CommonMind Consortium provides transcriptomic and epigenomic data for Schizophrenia and Bipolar Disorder', *Sci Data*, vol. 6, no. 1, p. 180, Sep. 2019.
- [103] M. I. Love, W. Huber, and S. Anders, 'Moderated estimation of fold change and dispersion for RNA-seq data with DESeq2', *Genome Biol*, vol. 15, no. 12, p. 550, Dec. 2014.
- [104] S. Hoops, S. Sahle, R. Gauges, C. Lee, J. Pahle, N. Simus, M. Singhal, L. Xu, P. Mendes, and U. Kummer, 'COPASI—a COMplex PATHway Simulator', *Bioinformatics*, vol. 22, no. 24, pp. 3067–3074, Dec. 2006.
- [105] M. T. J. Lowe, E. H. Kim, R. L. M. Faull, D. L. Christie, and H. J. Waldvogel, 'Dissociated expression of mitochondrial and cytosolic creatine kinases in the human brain: a new perspective on the role of creatine in brain energy metabolism', *J Cereb Blood Flow Metab*, vol. 33, no. 8, pp. 1295–1306, Aug. 2013.
- [106] T. Zheng, D. Kotol, R. Sjöberg, N. Mitsios, M. Uhlén, W. Zhong, F. Edfors, and J. Mulder, 'Characterization of reduced astrocyte creatine kinase levels in Alzheimer's disease', *Glia*, vol. 72, no. 9, pp. 1590–1603, Sep. 2024.
- [107] R. H. Andres, A. D. Ducray, U. Schlattner, T. Wallimann, and H. R. Widmer, 'Functions and effects of creatine in the central nervous system', *Brain Research Bulletin*, vol. 76, no. 4, pp. 329–343, Jul. 2008.
- [108] E. Wyatt, R. Wu, W. Rabeh, H.-W. Park, M. Ghanefar, and H. Ardehali, 'Regulation and Cytoprotective Role of Hexokinase III', *PLoS ONE*, vol. 5, no. 11, p. e13823, Nov. 2010.
- [109] G. A. Dunaway, T. P. Kasten, T. Sebo, and R. Trapp, 'Analysis of the phosphofructokinase subunits and isoenzymes in human tissues', *Biochem J*, vol. 251, no. 3, pp. 677–683, May 1988.
- [110] J.-H. Lee, R. Liu, J. Li, C. Zhang, Y. Wang, Q. Cai, X. Qian, Y. Xia, Y. Zheng, Y. Piao, Q. Chen, J. F. de Groot, T. Jiang, and Z. Lu, 'Stabilization of phosphofructokinase 1 platelet isoform by AKT promotes tumorigenesis', *Nat Commun*, vol. 8, no. 1, p. 949, Oct. 2017.

- [111] Y. Wei, M. Lu, M. Mei, H. Wang, Z. Han, M. Chen, H. Yao, N. Song, X. Ding, J. Ding, M. Xiao, and G. Hu, 'Pyridoxine induces glutathione synthesis via PKM2-mediated Nrf2 transactivation and confers neuroprotection', *Nat Commun*, vol. 11, no. 1, p. 941, Feb. 2020.
- [112] N.-M. Wilpert, M. Krueger, R. Opitz, D. Sebinger, S. Paisdzior, B. Mages, A. Schulz, J. Spranger, E. K. Wirth, H. Stachelscheid, P. Mergenthaler, P. Vajkoczy, H. Krude, P. Kühnen, I. Bechmann, and H. Biebermann, 'Spatiotemporal Changes of Cerebral Monocarboxylate Transporter 8 Expression', *Thyroid*, vol. 30, no. 9, pp. 1366–1383, Sep. 2020.
- [113] K. Banki, E. Colombo, F. Sia, D. Halladay, D. H. Mattson, A. H. Tatum, P. T. Massa, P. E. Phillips, and A. Perl, 'Oligodendrocyte-specific expression and autoantigenicity of transaldolase in multiple sclerosis', *J Exp Med*, vol. 180, no. 5, pp. 1649–1663, Nov. 1994.
- [114] A. K. Frame, J. W. Robinson, N. H. Mahmoudzadeh, J. M. Tennessen, A. F. Simon, and R. C. Cumming, 'Aging and memory are altered by genetically manipulating lactate dehydrogenase in the neurons or glia of flies', *Aging (Albany NY)*, vol. 15, no. 4, pp. 947–981, Feb. 2023.
- [115] A. E. Grams, I. Brote, S. Maderwald, K. Kollia, M. E. Ladd, M. Forsting, and E. R. Gizewski, 'Cerebral Magnetic Resonance Spectroscopy at 7 Tesla', *Academic Radiology*, vol. 18, no. 5, pp. 584–587, May 2011.
- [116] A. Rietzler, R. Steiger, S. Mangesius, L.-M. Walchhofer, R. M. Gothe, M. Schocke, E. R. Gizewski, and A. E. Grams, 'Energy metabolism measured by ³¹P magnetic resonance spectroscopy in the healthy human brain', *Journal of Neuroradiology*, vol. 49, no. 5, pp. 370–379, Sep. 2022.
- [117] C. He, S. Rong, P. Zhang, R. Li, X. Li, Y. Li, L. Wang, and Y. Zhang, 'Metabolite changes in prefrontal lobes and the anterior cingulate cortex correlate with processing speed and executive function in Parkinson disease patients', *Quant Imaging Med Surg*, vol. 12, no. 8, pp. 4226–4238, Aug. 2022.
- [118] D. Martins-de-Souza, W. F. Gattaz, A. Schmitt, C. Rewerts, G. Maccarrone, E. Dias-Neto, and C. W. Turck, 'Prefrontal cortex shotgun proteome analysis reveals altered calcium homeostasis and immune system imbalance in schizophrenia', *Eur Arch Psychiatry Clin Neurosci*, vol. 259, no. 3, pp. 151–163, Apr. 2009.
- [119] S. I. Novikova, F. He, N. J. Cutrufello, and M. S. Lidow, 'Identification of protein biomarkers for schizophrenia and bipolar disorder in the postmortem prefrontal cortex using SELDI-TOF-MS ProteinChip profiling combined with MALDI-TOF-PSD-MS analysis', *Neurobiol Dis*, vol. 23, no. 1, pp. 61–76, Jul. 2006.
- [120] J. A. English, P. Dicker, M. Föcking, M. J. Dunn, and D. R. Cotter, '2-D DIGE analysis implicates cytoskeletal abnormalities in psychiatric disease', *Proteomics*, vol. 9, no. 12, pp. 3368–3382, Jun. 2009.
- [121] K.-H. Smalla, M. Mikhaylova, J. Sahin, H.-G. Bernstein, B. Bogerts, A. Schmitt, R. van der Schors, A. B. Smit, K. W. Li, E. D. Gundelfinger, and M. R. Kreutz, 'A comparison of the synaptic proteome in human chronic schizophrenia and rat ketamine psychosis suggest that prohibitin is involved in the synaptic pathology of schizophrenia', *Mol Psychiatry*, vol. 13, no. 9, pp. 878–896, Sep. 2008.

- [122] D. Martins-de-Souza, W. F. Gattaz, A. Schmitt, G. Maccarrone, E. Hunyadi-Gulyás, M. N. Eberlin, G. H. M. F. Souza, S. Marangoni, J. C. Novello, C. W. Turck, and E. Dias-Neto, 'Proteomic analysis of dorsolateral prefrontal cortex indicates the involvement of cytoskeleton, oligodendrocyte, energy metabolism and new potential markers in schizophrenia', *J Psychiatr Res*, vol. 43, no. 11, pp. 978–986, Jul. 2009.
- [123] C. Panayiotou, N. Solaroli, and A. Karlsson, 'The many isoforms of human adenylate kinases', *The International Journal of Biochemistry & Cell Biology*, vol. 49, pp. 75–83, Apr. 2014.
- [124] H. Park, T.-I. Kam, Y. Kim, H. Choi, Y. Gwon, C. Kim, J.-Y. Koh, and Y.-K. Jung, 'Neuropathogenic role of adenylate kinase-1 in A β -mediated tau phosphorylation via AMPK and GSK3 β ', *Human Molecular Genetics*, vol. 21, no. 12, pp. 2725–2737, Jun. 2012.
- [125] G. Sh. Burbaeva, O. K. Savushkina, and I. S. Boksha, 'Creatine kinase BB in brain in schizophrenia', *The World Journal of Biological Psychiatry*, vol. 4, no. 4, pp. 177–183, Jan. 2003.
- [126] T. P. Klushnik, A. Ya. Spunde, A. G. Yakovlev, Z. A. Khuchua, V. A. Saks, and M. E. Vartanyan, 'Intracellular alterations of the creatine kinase isoforms in brains of schizophrenic patients', *Molecular and Chemical Neuropathology*, vol. 15, no. 3, pp. 271–280, Dec. 1991.
- [127] A. T. Behan, C. Byrne, M. J. Dunn, G. Cagney, and D. R. Cotter, 'Proteomic analysis of membrane microdomain-associated proteins in the dorsolateral prefrontal cortex in schizophrenia and bipolar disorder reveals alterations in LAMP, STXBP1 and BASP1 protein expression', *Mol Psychiatry*, vol. 14, no. 6, pp. 601–613, Jun. 2009.
- [128] D. Clark, I. Dedova, S. Cordwell, and I. Matsumoto, 'A proteome analysis of the anterior cingulate cortex gray matter in schizophrenia', *Mol Psychiatry*, vol. 11, no. 5, pp. 459–470, 423, May 2006.
- [129] D. Clark, I. Dedova, S. Cordwell, and I. Matsumoto, 'Altered proteins of the anterior cingulate cortex white matter proteome in schizophrenia', *Proteomics Clin Appl*, vol. 1, no. 2, pp. 157–166, Feb. 2007.
- [130] D. Martins-de-Souza, A. Schmitt, R. Röder, M. Lebar, T. Schneider-Axmann, P. Falkai, and C. W. Turck, 'Sex-specific proteome differences in the anterior cingulate cortex of schizophrenia', *J Psychiatr Res*, vol. 44, no. 14, pp. 989–991, Oct. 2010.
- [131] E. O. Voit, 'The best models of metabolism', *WIREs Mechanisms of Disease*, vol. 9, no. 6, p. e1391, Nov. 2017.
- [132] L. Townsend, T. Pillinger, P. Selvaggi, M. Veronese, F. Turkheimer, and O. Howes, 'Brain glucose metabolism in schizophrenia: a systematic review and meta-analysis of 18FDG-PET studies in schizophrenia', *Psychol Med*, vol. 53, no. 11, pp. 4880–4897, Aug. 2023.

APPENDIX 1: BRAIN ENERGY METABOLISM MODELS

The table presented in this appendix exhibits some of the most relevant brain energy metabolism models found from the literature. Note that the list is not a comprehensive list of all existing brain energy metabolism models. The references marked with an asterisk (*) are not presented in the table but are listed in the references below.

TABLE REFERENCES

- A. Aubert, R. Costalat, and R. Valabrègue, Modelling of the coupling between brain electrical activity and metabolism, *Acta Biotheor*, vol. 49, no. 4, pp. 301–26, Dec. 2001.
- *A. Aubert and R. Costalat, A model of the coupling between brain electrical activity, metabolism and hemodynamics: application to the interpretation of functional neuroimaging, *NeuroImage*, vol. 17, no. 3, pp. 1162–81, Nov. 2002.
- A. Aubert and R. Costalat, Interaction between Astrocytes and Neurons Studied using a Mathematical Model of Compartmentalized Energy Metabolism. *Journal of Cerebral Blood Flow & Metabolism*, vol. 25, no. 11, pp. 1476-1490, Nov. 2005
- *A. Aubert, R. Costalat, P.J. Magistretti, and L. Pellerin, Brain lactate kinetics: Modeling evidence for neuronal lactate uptake upon activation, *Proc Natl Acad Sci U S A*, vol. 102, no. 45, pp. 16448-53, Nov. 2005.
- *A. Aubert, L. Pellerin, P.J. Magistretti, and R. Costalat, A coherent neurobiological framework for functional neuroimaging provided by a model integrating compartmentalized energy metabolism, *Proc Natl Acad Sci U S A*, vol. 104, no. 10, pp. 4188-93, Mar. 2007.
- D. Calvetti, Y. Cheng, and E. Somersalo, A spatially distributed computational model of brain cellular metabolism, *J Theor Biol*, vol. 376, no. 7, pp. 48-65, Jul. 2015.
- D. Calvetti, G. Capo Rangel, L. Gerardo Giorda, and E. Somersalo, A computational model integrating brain electrophysiology and metabolism highlights the key role of extracellular potassium and oxygen, *J Theor Biol*, vol. 446, no. 7, pp. 238-258, Jun. 2018.
- M. Cloutier, F.B. Bolger, J.P. Lowry, and P. Wellstead, An integrative dynamic model of brain energy metabolism using in vivo neurochemical measurements, *J Comput Neurosci*, vol. 27, no. 3, pp. 391-414, Dec. 2009.
- M. DiNuzzo, S. Mangia, B. Maraviglia, and F. Giove, Changes in glucose uptake rather than lactate shuttle take center stage in subserving neuroenergetics: evidence from mathematical modeling, *J Cereb Blood Flow Metab*, vol. 30, no. 3, pp. 586-602, Mar. 2010.
- M. DiNuzzo, F. Giove, B. Maraviglia, and S. Mangia, Computational Flux Balance Analysis Predicts that Stimulation of Energy Metabolism in Astrocytes and their Metabolic Interactions with Neurons Depend on Uptake of K⁺ Rather than Glutamate, *Neurochem Res*, vol. 42, no. 1, pp. 202-216, Jan. 2017.
- *R. Heinrich, S. Schuster, The regulation of cellular systems, 1st ed, Boston, MA, Springer US, 1996.
- R. Jolivet, J.S. Coggan, I. Allaman, and P.J. Magistretti, Multi-timescale modeling of activity-dependent metabolic coupling in the neuron-glia-vasculature ensemble, *PLoS Comput Biol*, vol. 11, no. 2, p. e1004036, Feb. 2015.
- S. Mangia, I.A. Simpson, S.J. Vannucci, and A. Carruthers, The in vivo neuron-to-astrocyte lactate shuttle in human brain: evidence from modeling of measured lactate levels during visual stimulation, *J Neurochem*, Suppl 1 (Suppl 1), pp. 55-62, May 2009.
- R. Occhipinti, E. Somersalo, and D. Calvetti, Astrocytes as the glucose shunt for glutamatergic neurons at high activity: an in silico study, *J Neurophysiol*, vol. 101, no. 5, pp. 2528-38, May 2009.
- I.A. Simpson, A. Carruthers, and S.J. Vannucci, Supply and demand in cerebral energy metabolism: the role of nutrient transporters, *J Cereb Blood Flow Metab*, vol. 27, no. 11, pp. 1766-91, Nov. 2007.
- F. Winter, C. Bludszweit-Philipp, and O. Wolkenhauer, Mathematical analysis of the influence of brain metabolism on the BOLD signal in Alzheimer's disease, *J Cereb Blood Flow Metab*, vol. 38, no. 2, pp. 304-316, Feb. 2018.

Authors	Expands on	What is modelled	Number of equations	Compartments	Model file available	Simulator
Aubert–Costalat models						
Aubert et al. (2001)		Neuronal energy metabolism, brain hemodynamics, and transport of ions and metabolites	32			
Aubert & Costalat (2005)	Aubert et al. (2001), Aubert & Costalat (2002)*	Compartmentalized energy metabolism of neurons and astrocytes, brain hemodynamics, transport of ions and metabolites	43	Neuron, astrocyte, extracellular space, capillary	Yes, BioModels database ID: MODEL1411210000 (SBML format)	Unknown
Cloutier et al. (2009)	Aubert & Costalat (2005), Aubert et al. (2005)*	Extends and refines Aubert & Costalat (2005) model, especially by adding glycogen dynamics in astrocytes	34	Neuron (cytosolic), neuron (mitochondrial), astrocyte (cytosolic), astrocyte (mitochondrial), extracellular space, capillary	Yes, BioModels database ID: MODEL1006230041 (SBML format + Copasi file)	MATLAB and the Systems Biology toolbox
Jolivet et al. (2015)	Aubert & Costalat (2005), Aubert et al. (2007)*	Extends and refines Aubert & Costalat (2005) and Aubert et al. (2007) models, especially by adding mitochondrial compartments	33	Neuron, astrocyte, extracellular space, capillary	No	MATLAB
Winter et al. (2018)	Aubert & Costalat (2005), Cloutier et al. (2009), Heinrich & Schuster (1996)*	Extends and refines Aubert & Costalat (2005) and Cloutier et al. (2009) models, especially by adding pentose-phosphate pathway	64	Neuron, astrocyte, the extracellular space, capillary, artery, vein	Yes, BioModels database, ID: MODEL1603240000 (SBML format + Copasi file)	Copasi

Simpson–Mangia models

Simpson et al. (2007)	Very simple model focusing on transport of glucose and lactate between the compartments	10	Neuron, astrocyte, endothelium, basal lamina, interstitium	No	No
Mangia et al. (2009)	The model is the same as in Simpson et al. (2007), but <i>in vivo</i> human fMRS data was incorporated to the model	10	Neuron, astrocyte, endothelium, basal lamina, interstitium	No	4th order Runge Kutta Numerical Integration + Berkeley Madonna

Calvetti–Occhipinti–Somersalo models

Occhipinti, Somersalo and Calvetti (2007)	Detailed descriptions of glycolysis, TCA cycle, glutamine-glutamate and GABA shunts for neurons and astrocytes, substrate transports between the compartments	109	Neuron (cytosolic), neuron (mitochondrial), astrocyte (cytosolic), astrocyte (mitochondrial), blood (includes extracellular space)	No	MATLAB
Calvetti et al. (2015)	Improves earlier models by adding improved spatial distribution	34N + 4 (N = number of compartments)	Neuron, astrocyte, extracellular space, synaptic cleft, blood	No	Unknown
Calvetti et al. (2018)	Extends earlier models by combining the metabolic neuron/astrocyte dynamics with an electrophysiological model, and adding a two-way feedback system	30	Neuron, astrocyte, extracellular space, blood	No	MATLAB

DiNuzzo models

<p>DiNuzzo et al. (2010)</p>	<p>Aubert & Costalat (2002)*, Aubert & Costalat (2005), Simpson et al. (2007), Mangia et al. (2009)</p> <p>Involvement of neurons and astrocytes in the coupling between cerebral electrical activity, hemodynamics, and energy metabolism</p>	<p>56</p>	<p>Neuron, astrocyte, endothelium, interstitium, basal lamina, capillary, blood</p>	<p>No</p> <p>MATLAB</p>
<p>DiNuzzo et al. (2017)</p>	<p>Extends DiNuzzo et al. (2010) model by incorporating explicit pathways involved in ion homeostasis related to neurotransmission</p>	<p>119</p>	<p>Neuron (cytosolic), neuron (mitochondrial), neuron (synaptic vesicles), astrocyte (cytosolic), astrocyte (mitochondrial), extracellular space, capillary</p>	<p>Partly (The model is available in SBML-format in Supplementary material 2, but initial concentrations and reaction rate units are not provided)</p> <p>MATLAB.</p>

APPENDIX 2: THE R CODE

The R code presented below is for the prefrontal cortex (PFC) bulk RNA sequencing data set. The same analyses were done on the anterior cingulate cortex (ACC) data set. RStudio version 2024.04.2+764 and R version 4.4.1 were used to perform the analyses. The packages that were used are *BiocManager* (version 1.30.25), *DESeq2* (1.44.0), *AnnotationDbi* (1.66.0), *org.Hs.eg.db* (3.19.1), *tidyr* (1.3.1), *ggplot2* (3.5.1), *patchwork* (1.2.0) and *dplyr* (1.1.4).

DIFFERENTIAL EXPRESSION ANALYSIS

Importing the data

```
count_data <- read.delim(
  "/Users/ilonamakinen/Desktop/CommonMind_PFC_rawcounts.tsv",
  sep = "\t")
metadata <- read.delim(
  "/Users/ilonamakinen/Desktop/CommonMind_PFC_metadata.tsv",
  sep = "\t")
winter_genes <- unlist(read.delim(
  "/Users/ilonamakinen/Desktop/winter_genes.txt",
  header = FALSE,
  sep = "\t"))
```

Setting Ensembl IDs as rownames

```
row.names(count_data) <- count_data[ ,1]
count_data <- count_data[ , -1]
```

Filtering out genes whose expression is in the lowest 10%

```
row_sums <- rowSums(count_data)
low_exp_cutoff <- quantile(row_sums, probs = 0.10)
count_data_filtered <- count_data[rowSums(count_data[ ,]) >
  low_exp_cutoff, ]
```

Performing the differential expression (DE) analysis

```
DESeq_data_set <- DESeqDataSetFromMatrix(
  countData = count_data_filtered,
  colData = metadata,
  design = ~ Diagnosis + Age + Sex + PMI)
DESeq_data <- DESeq(DESeq_data_set)
```

Extracting the DE analysis results. Creating a data frame for easier inspection of results.

```
DESeq_result <- results(
```

```

DESeq_data,
contrast = c("Diagnosis", "SCZ", "HC"),
alpha = 0.01,
independentFiltering = TRUE)
DESeq_result_df <- results(
  DESeq_data,
  contrast = c("Diagnosis", "SCZ", "HC"),
  alpha = 0.01,
  independentFiltering = TRUE,
  tidy = TRUE)
summary(DESeq_result)

# Matching Ensembl IDs to gene symbols. First, version numbers must be
removed from the Ensembl IDs.
ensembl_ids_no_version <- gsub("\\..*", "", row.names(DESeq_result))
rownames(DESeq_result) <- ensembl_ids_no_version
DESeq_result_df$row <- ensembl_ids_no_version

gene_symbols <- mapIds(
  org.Hs.eg.db,
  keys = row.names(DESeq_result),
  keytype = "ENSEMBL",
  column = "SYMBOL",
  multiVals = "first")

# NA values are replaced with "NA" string, so they can be used as
rownames
gene_symbols[is.na(gene_symbols)] <- "NA"
rownames(DESeq_result) <- gene_symbols
DESeq_result_df$gene_symbol <- gene_symbols

# Extracting the genes which are in the Winter gene list
in_gene_list <- DESeq_result[rownames(DESeq_result) %in%
  winter_genes, ]
in_gene_list_df <- DESeq_result_df[DESeq_result_df$gene_symbol %in%
  winter_genes,]
summary(in_gene_list)

# CREATING MIXTURE FILE FOR CIBERSORTX

# Extracting DESeq2 normalized counts and matching EnsemblIDs to gene
symbols
DESeq_normalized_counts <- as.data.frame(counts(DESeq_data,
normalized=T))
DESeq_normalized_counts$gene_symbol <- gene_symbols

```

```

# Removing NA values and formatting the data frame
DESeq_normalized_counts_noNA <- na.omit(
  DESeq_normalized_counts,
  cols = "gene_symbol")
DESeq_normalized_counts_noNA <- DESeq_normalized_counts_noNA[ ,
  c(ncol(DESeq_normalized_counts_noNA),
  1:(ncol(DESeq_normalized_counts_noNA)-1))]
DESeq_normalized_counts_noNA <- DESeq_normalized_counts_noNA[, -483]

# Writing the mixture file
write.table(DESeq_normalized_counts_noNA,
  file = "mixture_file_ACC_DESeq2.txt",
  sep = "\t",
  row.names = FALSE,
  col.names = TRUE,
  quote = FALSE)

# CALCULATING COEFFICIENTS USING BULK DATA

# Extracting the genes of interest. Note that these genes are for PFC
data. The genes of interest are different for ACC data.
genes_of_interest <- c("CKB", "PFKM", "PGLS", "PKM", "RPE")
in_genes_of_interest_df <- DESeq_normalized_counts[
  DESeq_normalized_counts$gene_symbol %in% genes_of_interest, ]

# Separating SCZ samples from HC samples and calculating mean
expression values for each gene in both groups. Note that the column
numbers are different in PFC and ACC data sets.
scz_indices <- which(metadata$Diagnosis == "SCZ")
hc_indices <- which(metadata$Diagnosis == "HC")

scz_counts <- in_genes_of_interest_df[,c(scz_indices, 559)]
hc_counts <- in_genes_of_interest_df[,c(hc_indices, 559)]

scz_counts$row_mean <- rowMeans(scz_counts[, -264])
hc_counts$row_mean <- rowMeans(hc_counts[-296])

# Calculating the coefficients for each gene of interest
scz_counts$multipliers <- scz_counts$row_mean / hc_counts$row_mean

# CALCULATING COEFFICIENTS USING CIBERSORTX IMPUTED EXPRESSIONS

```

```

# Importing cell-type specific data for neurons and astrocytes
astrocyte_df <- read.delim("/Users/ilonamakinen/Desktop/
  CIBERSORTxHiRes_Job16_Astrocytes_Window20.txt",
  sep = "\t")
neuron_df <- read.delim("/Users/ilonamakinen/Desktop/
  CIBERSORTxHiRes_Job16_Neurons_Window20.txt",
  sep = "\t")

# Extracting the genes of interest separately for both cell types.
Note that these genes are specific for PFC data, ACC data has
different genes of interest.
in_genes_of_interest_astro <- astrocyte_df[astrocyte_df$GeneSymbol ==
  "PGLS", ]
in_genes_of_interest_neuron <- neuron_df[neuron_df$GeneSymbol %in%
  c("PFKM", "PGLS", "PKM"), ]

# Moving the "GeneSymbol" column as the last column of the data frame
to get sample indices to match
in_genes_of_interest_astro <- in_genes_of_interest_astro[ ,
  c(2:ncol(in_genes_of_interest_astro), 1)]
in_genes_of_interest_neuron <- in_genes_of_interest_neuron[ ,
  c(2:ncol(in_genes_of_interest_neuron), 1)]

# Separating SCZ samples from HC samples and calculating mean
expression values for each gene in both groups. Note that the column
numbers are different in PFC and ACC data sets.
scz_counts_astro <- in_genes_of_interest_astro[ ,scz_indices]
hc_counts_astro <- in_genes_of_interest_astro[ ,hc_indices]

scz_counts_neuron <- in_genes_of_interest_neuron[ ,scz_indices]
hc_counts_neuron <- in_genes_of_interest_neuron[ ,hc_indices]

scz_counts_astro$row_mean <- rowMeans(scz_counts_astro)
hc_counts_astro$row_mean <- rowMeans(hc_counts_astro)

scz_counts_neuron$row_mean <- rowMeans(scz_counts_neuron)
hc_counts_neuron$row_mean <- rowMeans(hc_counts_neuron)

# Calculating the coefficients for each gene of interest
scz_counts_astro$multipliers <- scz_counts_astro$row_mean /
  hc_counts_astro$row_mean
scz_counts_neuron$multipliers <- scz_counts_neuron$row_mean /
  hc_counts_neuron$row_mean

```

```

# PLOTTING THE COPASI SIMULATION RESULTS

# Here, plotting of normalized concentrations based on PFKM
simulations is shown as an example. The absolute and normalized
concentrations were plotted using the same code for the rest of the
genes as well.

# Importing the concentration files
control <- read.table("/Users/ilonamakinen/Desktop/Copasi_files/
  Winter_control/control_concentrations.txt", header = TRUE)
PFK_neurons_CIBERSORT <- read.table("/Users/ilonamakinen/Desktop/
  Copasi_files/PFK_neurons_CIBERSORT/
  PFK_neurons_CIBERSORT_concentrations.txt", header = TRUE)
PFK_neurons_BULK <- read.table("/Users/ilonamakinen/Desktop/
  Copasi_files/PFK_neurons_BULK/
  PFK_neurons_BULK_concentrations.txt", header = TRUE)

# Normalizing the concentrations for easier inspection and comparison
of the plots
control_baselines <- control[1, -1]
CIBERSORT_baselines <- PFK_neurons_BULK[1, -1]
bulk_baselines <- PFK_neurons_CIBERSORT[1, -1]

control_normalized <- control
for (i in 1:25) {
  control_normalized[, i+1]
  <- control[, i+1] / control_baselines[1,i]
}

CIBERSORT_normalized <- PFK_neurons_CIBERSORT
for (i in 1:25) {
  CIBERSORT_normalized[, i+1]
  <- PFK_neurons_CIBERSORT[, i+1] / scz_baselines[1,i]
}

bulk_normalized <- PFK_neurons_BULK
for (i in 1:25) {
  bulk_normalized[, i+1]
  <- PFK_neurons_BULK[, i+1] / scz_baselines[1,i]
}

#Adjusting the time columns so that stimulus is at t=0
control_normalized$Time <- control_normalized$Time -
  (29900 + abs(-100))
CIBERSORT_normalized$Time <- CIBERSORT_normalized$Time -
  (29900 + abs(-100))
bulk_normalized$Time <- bulk_normalized$Time - (29900 + abs(-100))

```

```

# Combining the three data frames into one before plotting
control_normalized$group <- "Control"
bulk_normalized$group <- "SCZ (bulk)"
CIBERSORT_normalized$group <- "SCZ (CIBERSORTx)"

combined_data <- bind_rows(control_normalized, bulk_normalized,
  CIBERSORT_normalized)

combined_data_long <- combined_data %>% pivot_longer(
  cols = c(X.ATP.astrocytes., X.GLC.astrocytes.,
    X.LAC.astrocytes., X.PYR.astrocytes., X.NAD.astrocytes.,
    X.NADH.astrocytes., X.ATP.neurons., X.GLC.neurons.,
    X.LAC.neurons., X.PYR.neurons., X.NAD.neurons.,
    X.NADH.neurons.),
  names_to = "concentration_type",
  values_to = "concentration")

# Defining the order of the subplots with levels and the titles of the
subplots with labels
combined_data_long$concentration_type <- factor(
  combined_data_long$concentration_type,
  levels = c("X.ATP.astrocytes..", "X.GLC.astrocytes..",
    "X.LAC.astrocytes..", "X.PYR.astrocytes..",
    "X.NAD.astrocytes..", "X.NADH.astrocytes..", "X.ATP.neurons..",
    "X.GLC.neurons..", "X.LAC.neurons..", "X.PYR.neurons..",
    "X.NAD.neurons..", "X.NADH.neurons.."),
  labels = c("ATP astro", "GLC astro", "LAC astro", "PYR astro",
    "NAD astro", "NADH astro", "ATP neuron", "GLC neuron",
    "LAC neuron", "PYR neuron", "NAD neuron", "NADH neuron"))

# Plotting the concentrations of all metabolites into 12 subplots
ggplot(combined_data_long, aes(
  x = Time, y = concentration, color = group)) +
  geom_line() +
  facet_wrap(~ concentration_type, ncol = 6, scales = "free_y") +
  labs(x = "Time (s)", y = "Concentration (mmol/ml)") +
  scale_color_manual(values = c("Control" = "blue",
    "SCZ (CIBERSORTx)" = "orange", "SCZ (bulk)" = "red")) +
  theme(legend.position = "top", legend.title = element_blank(),
    panel.spacing = unit(1, "lines"))

```